PB161589

NBS

# Technical Note No. 88

## Boulder Laboratories

# PROLONGED SPACE-WAVE FADEOUTS IN TROPOSPHERIC PROPAGATION

BY

A. P. BARSIS AND MARY ELLEN JOHNSON

U. S. DEPARTMENT OF COMMERCE
NATIONAL BUREAU OF STANDARDS

## THE NATIONAL BUREAU OF STANDARDS

### Functions and Activities

The functions of the National Bureau of Standards are set forth in the Act of Congress, March 3, 1901, as amended by Congress in Public Law 619, 1950. These include the development and maintenance of the national standards of measurement and the provision of means and methods for making measurements consistent with these standards: the determination of physical constants and properties of materials: the development of methods and instruments for testing materials, devices, and structures; advisory services to government agencies on scientific and technical problems; invention and development of devices to serve special needs of the Government; and the development of standard practices, codes, and specifications. The work includes basic and applied research, development, engineering, instrumentation, testing, evaluation, calibration services, and various consultation and information services. Research projects are also performed for other government agencies when the work relates to and supplements the basic program of the Bureau or when the Bureau's unique competence is required. The scope of activities is suggested by the listing of divisions and sections on the inside of the back cover.

### Publications

The results of the Bureau's work take the form of either actual equipment and devices or published papers. These papers appear either in the Bureau's own series of publications or in the journals of professional and scientific societies. The Bureau itself publishes three periodicals available from the Government Printing Office: The Journal of Research, published in four separate sections, presents complete scientific and technical papers; the Technical News Bulletin presents summary and preliminary reports on work in progress; and Basic Radio Propagation Predictions provides data for determining the best frequencies to use for radio communications throughout the world. There are also five series of nonperiodical publications: Monographs, Applied Mathematics Series, Handbooks, Miscellaneous Publications, and Technical Notes.

Information on the Bureau's publications can be found in NBS Circular 460, Publications of the National Bureau of Standards ($1.25) and its Supplement ($1.50), available from the Superintendent of Documents, Government Printing Office, Washington 25, D.C.

# NATIONAL BUREAU OF STANDARDS

## *Technical Note*

88

February 8, 1961

# PROLONGED SPACE-WAVE FADEOUTS IN TROPOSPHERIC PROPAGATION

by

A. P. Barsis and Mary Ellen Johnson

NBS Technical Notes are designed to supplement the Bureau's regular publications program. They provide a means for making available scientific data that are of transient or limited interest. Technical Notes may be listed or referred to in the open literature. They are for sale by the Office of Technical Services, U. S. Department of Commerce, Washington 25, D. C.

DISTRIBUTED BY

UNITED STATES DEPARTMENT OF COMMERCE

OFFICE OF TECHNICAL SERVICES

WASHINGTON 25, D. C.

Price $2.00

TABLE OF CONTENTS

## ABSTRACT

This paper contains the results of studies performed during the last several years on the short-term variability of tropospheric signals received over within-the-horizon paths. Signal variations of this type have been termed "prolonged space-wave fadeouts," as they are mainly characterized by reductions in signal level to many decibels below presumably constant values determined from geometrical optics methods. The data described here were obtained from measurements over propagation paths in the Pacific Coast region of Southern California, and the continental region of Eastern Colorado. Fadeouts are analyzed as a function of carrier frequency, path characteristics, and meteorological parameters. The study also includes an evaluation of fadeouts observed over a path using a mountain peak as a diffracting knife-edge like obstacle between transmitter and receiver.

# PROLONGED SPACE-WAVE FADEOUTS IN TROPOSPHERIC PROPAGATION

by

A. P. Barsis and M. E. Johnson

## 1. INTRODUCTION

The short-term variability of long-distance beyond-the-horizon signals in the very-high and ultra-high frequency bands can easily be described statistically. It has been postulated by scattering theories and verified experimentally that the short-term variations of such signals are Rayleigh-distributed. Short-term as used here means periods of up to one hour. However, this relatively simple statistical description does not apply to within-the-horizon, or diffraction paths. Inspection of field strength recordings shows that short-term signal variations over such paths consist of "fadeouts," i.e. reductions in signal level to values below a long-term average or median, which may last from minutes to a good part of the hour. The term "space-wave fadeout" was chosen because the phonomenon was first observed over within-the-horizon paths at ultra-high frequencies, where the space-wave (presumably constant for a standard atmosphere) is the principal mode of propagation.

A description and evaluation of the initial National Bureau of Standards fadeout studies is given in a paper by Bean [1954], where a relation between the occurrence of ground based layers and fadeouts was first extablished. Recently the same phenomenon was observed over a "knife-edge diffraction" path, which uses a mountain as the diffracting obstacle between the path terminals.

The following data are included in this study:

1. Data obtained over the 113 km path in Eastern Colorado which already have been discussed by Bean in his original paper [1954]. The experiments were performed by the National Bureau of Standards in 1952 and 1953, using a frequency of 1046 Mc. The path profile is shown in Fig. 1.
2. Data obtained from the Navy Electronics Laboratory. The experiments were performed over a 185 km path in Southern California during 1950 and 1951, using frequencies of 138 and 1250 Mc. The path profile is shown in Fig. 2.
3. Data obtained from a joint program by the National Bureau of Standards and the Naval Air Missile Test Center (Pt. Mugu, California). A 104 km over-water path in Southern California was used during the period November 1955 to July 1959, with frequencies in the 100, 250, and 400 Mc range. The path profile is shown in Fig. 3. Some results have been presented in an earlier paper by Barsis and Capps [1957].
4. Data obtained from a 223 km path in Colorado, using Pikes Peak as a diffracting knife-edge. The experiments were performed by the National Bureau of Standards in 1959 and 1960, using a frequency of 751 Mc. The path profile is shown in Fig. 4.

Pertinent data for all paths are shown on Table I, below. They include the terminal elevation, grazing angles, and other characteristics. The grazing angles are given for an effective earth radius of 9000 km. This value corresponds approximately to the 4/3 effective earth radius

factor commonly used. For the exponential model of atmospheric radio refractivity [Bean and Thayer, 1959a], the corresponding value of surface refractivity is approximately 316 N-units.

TABLE I

Characteristics of Paths Used for Fadeout Studies

| Path | Length km | Terminal Heights, Meters above ground | Terminal Heights, Meters above m.s.l. | Grazing Angle for N = 316 milliradians |
|---|---|---|---|---|
| Cheyenne Mountain - Karval | 113 | * 1.5, 4.3 & 13 | 2670 1545, 1547 & 1555 | 3.6, 3.7 & 4.0 |
| Mt. Wilson - Pt. Loma | 185 | * * | 1712 30 | 3.8 |
| San Nicolas Island - Laguna Peak | 104 | 6 * | 264 254 & 427 | 2.0 & 3.6 |
| Beulah - Table Mesa | 223 | 7 8 & 15 | 1912 1674 & 1681 | 4292m** |

* Not pertinent, because on mountain top or above steep slope.
** Height of obstacle above mean sea level.

| Path | Carrier Frequency Used, Mc | Polarization | Period of Operation |
|---|---|---|---|
| Cheyenne Mountain - Karval | 1046 | Horizontal | 1952-53 |
| Mt. Wilson - Pt. Loma | 138, 1250 | Not known | 1950-51 |
| San Nicolas Island - Laguna Peak | 98.6, 100, 244 249, 394 | Vertical | 1955-59 |
| Beulah - Table Mesa | 751 | Horizontal | 1959-60 |

In order to provide a unique definition for the phenomenon to be studied, it is necessary to emphasize the distinction between the term "fading" as commonly employed, and the term "prolonged space-wave fadeout" as used here. "Fading" usually refers to the rapid amplitude variations of a radio signal transmitted over relatively long distances through the troposphere or the ionosphere. In the case of long-distance tropospheric scatter propagation, the rapid fading is presumably caused by the vector addition of a large number of field components arriving at the receiving location with random phase. The amplitude distribution of such a signal tends to have the form of a Rayleigh distribution, and the fading rate with reference to a short-term average or median value varies with carrier frequency, atmospheric conditions, and path length approximately within the limits of 0.1 to 10 cycles per second.

The term "prolonged space-wave fadeout," however, is restricted to paths where the geometric-optics space-wave is predominant and to knife-edge diffraction paths. The fading rate here is extremely slow, and the amplitude distribution of the received signal cannot be represented by a Rayleigh, or any other simple distribution function. Fadeouts of this type may be caused by vector addition of a few specular components caused by reflection from layers, or similar phenomena, and tend to shift with the variable refractive index structure of the lower atmosphere, thus causing the variations in signal level. Possible small contributions to the received field due to scatter are neglected in this analysis. Fig. 5 shows a typical space-wave fadeout. The depth D of the fadeout is measured with reference to an arbitrary signal level, which may be an hourly median value, or a long-term median of hourly median values. The same reference level is R decibels above the RMS receiver noise level. The quantity

$$R_D = R - D \qquad (1)$$

is then the instantaneous carrier envelope signal to RMS noise ratio, and can be used to calculate quantities like teleprinter error rate for signals of this character.

The definition of space-wave fadeouts was restricted to those fadeouts which extend to at least 5 decibels below the reference level. In earlier analyses (Cheyenne Mountain - Karval, Mt. Wilson - Point Loma, and some of the Point Mugu data) fadeouts of a duration less than one minute at the 5 db level were neglected due to the time-scale of the records analyzed. This restriction was removed in later analyses, where it was possible to measure fadeouts of shorter durations.

Fadeout statistics to be discussed in this paper include the fadeout incidence, which is the number of fadeouts observed in a given time period, the diurnal and seasonal variation in fadeout incidence and other characteristics, and the distribution of fadeout durations at various levels. In all cases, distributions of fadeout durations were obtained by setting up convenient time intervals (like 1-2 minutes, 2-3 minutes, etc.), counting the number of fadeouts whose duration fell into each interval, and calculating a cumulative distribution in percent of the total number of fadeouts. For the Pt. Mugu data, extensive meteorological observations are available, which permit an analysis of fadeout characteristics as functions of meteorological parameters. In most cases a comparison of fadeout characteristics for various values of carrier frequency is also included.

## 2. EASTERN COLORADO DATA

### 2.1 General

Description of the tropospheric propagation paths extending eastward from Cheyenne Mountain is contained in a National Bureau of Standards Circular [Barsis, et al, 1955]. Of the paths investigated,

the one to Karval was used for fadeout studies on 1046 Mc. The path length is 113 kilometers and the path profile is shown on Fig. 1. Results obtained in 1952 have already been reported by Bean [1954]. From his analysis of fadeout dependence on meteorological characteristics he concluded that fadeouts were more likely when a ground-modified refractive index profile was observed, than for a well-mixed atmosphere with a linear profile.

Additional data were obtained during 1953, including simultaneous measurements at Karval in December using three dipole antennas at 1.5, 4.3 and 13 meters above ground. This corresponds to spacings up to approximately 30 wavelengths. Fig. 6 shows a sample of recording charts for the three antenna heights at the time of a fadeout. It appears that the fadeout characteristics are extremely well correlated in time. The "transmitter-off" period in the record serves to emphasize the time correlation of the fadeouts. The small, more rapid signal variations superimposed on the recording traces are probably due to a scatter component, and are not considered in the analysis.

## 2.2 Continuous Recordings 1952-1953

An antenna 13 meters above ground was used for continuous recordings during both years. Fig. 7 shows the fadeout incidence (number of occurrences of fadeouts) as a function of the time of the day for all data and for both years. The values shown refer to the 5 db fadeouts, and the abscissa scale is normalized to take into account times of equipment outage. A very definite diurnal trend is evident: fadeouts are much more numerous during the night and early morning hours. The minimum number of fadeouts was observed around noon and in the early afternoon. The possible cause for this diurnal behavior and the

correlation of fadeouts with ground modifications of the refractive index profile has been discussed by Bean [1954].

An interesting example of this correlation is shown on Fig. 8. Here, the refractivity profiles observed in the same area have been plotted versus the time of the day together with the observed fadeout incidence. The data shown are for December 13, 1953. Refractivity profiles were obtained along the 500-ft tower at Haswell, some 38 km to the southeast of the Karval site. For this day, fadeouts were observed only during the early morning hours, when the refractivity profile showed a marked ground modification. Coincidentally, the surface refractivity during these hours was near its daily minimum, as also shown on Fig. 8.

Seasonal variations of fadeout incidence at Karval are shown on Figs. 9 and 10. Fig. 9 is a bar graph similar to Fig. 7, but showing the normalized 5 db fadeout incidence for the months from February 1952 to August 1953. Fig. 10 shows the seasonal variations of total fadeout time at the 5 db and 10 db levels relative to the monthly transmission loss median for the same time period. This is the total time per month during which the signal remained at or below these levels, expressed as a fraction of the total recording time. Both graphs demonstrate that fadeouts are much more numerous in summer than in winter, as the summer maximum exists for both years.

Thus the results of the diurnal and seasonal variation analysis shows that for the relatively dry continental climate of Eastern Colorado, fadeouts tend to be more numerous in summer than in winter, and more numerous at night time than during daylight hours.

A somewhat different analysis of fadeout characteristics for this path is presented in the next two figures. Fig. 11 shows the cumulative distribution of fadeout durations at three levels with reference to the monthly median. Data for the entire period of recording during 1952

and 1953 were included in this study. From Fig. 11 it is seen that the median fadeout duration is 6.2 minutes at the 5 db level, 5.0 minutes at the 10 db level, and 3.1 minutes at the 15 db level below the monthly median transmission loss value. It also is seen, as an example, that 2% of all 10 db fadeouts are at least one hour (60 minutes) long. The importance of such statistics in the design of communication, navigation, or positioning systems is evident.

The data from Fig. 11 are replotted in a different fashion on Fig. 12. Here each curve represents a fixed percentage of all fadeouts observed, and thus shows the level distribution during individual fadeouts. The 50% curve on Fig. 12, as an example, represents the distributions of levels for the "median" fadeout. These curves have been extrapolated in order to obtain estimates for the duration of deep fades in excess of 15 db. The graph shows, as an example, that almost all fadeouts (as represented by the curve labelled 99%) have a duration of 0.43 minutes at a level of 25 db below the monthly median.

Curves of this type (Fig. 12) will be used for system performance calculations in a companion paper.

## 2.3 Vertical Diversity Studies

As mentioned above, simultaneous measurements using three receiving antenna heights were made at Karval during December, 1953. The receiving antennas were at 1.5, 4.3, and 14 meters above ground, and were connected to separate 1046 Mc receivers and recorders. During this period a total number of 322 hours were recorded simultaneously on all three receivers. The following table summarizes the 5 db and 10 db fadeout statistics for these hours.

TABLE II

Fadeout Statistics, Eastern Colorado Path

1046 Mc, December 1953

| Antenna Height above ground, meters | Fadeout Incidence | | | |
|---|---|---|---|---|
| | 5 db | | 10 db | |
| | Total Number of Fadeouts | Fadeouts per hour | Total Number of Fadeouts | Fadeouts per hour |
| 1.5 | 36 | 0.112 | 7 | 0.0217 |
| 4.3 | 30 | 0.093 | 5 | 0.0155 |
| 14.0 | 75 | 0.233 | 14 | 0.0435 |

It is seen that there are about twice as many fadeouts on the higher antenna than on the lower ones. For the purpose of estimating the effectiveness of vertical diversity, a study was made of the number of instances when 5 db and 10 db fadeouts occurred simultaneously on pairs of antennas or on all three of them. Simultaneous fadeouts mean that any portion of the fadeouts observed on the antennas considered coincided in time. Results are given in Table III, below.

TABLE III

Statistics of Simultaneous Fadeouts for December 1953

| Antenna Combinations | Number of Fadeouts Observed Simultaneously | |
|---|---|---|
| | 5 db | 10 db |
| 1.5 and 4.3 m | 25 | 5 |
| 1.5 and 14 m | 27 | 6 |
| 4.3 and 14 m | 24 | 5 |
| all antennas | 19 | 5 |

The numbers in Table III may be expressed as percentages of the total number of fadeouts observed on either one of the pair or triplet compared. This is done in Table IV, which follows. Here the designations "higher," "middle," and "lower" refer to the comparison of the combinations listed in the first column.

TABLE IV

Percentages of Fadeouts Observed Simultaneously on Two or More Antennas

| Antenna Combinations | Percentages of Total Number of Fadeouts Observed on Antenna | | |
|---|---|---|---|
| | Higher | Middle | Lower |
| | | 5 db Fadeouts | |
| 1.5 and 4.3 m | 83.3 | - | 69.4 |
| 1.5 and 14 m | 75.0 | - | 36.0 |
| 4.3 and 14 m | 80.0 | - | 32.0 |
| all antennas | 25.3 | 63.3 | 52.8 |
| | | 10 db Fadeouts | |
| 1.5 and 4.3 m | 100.0 | - | 71.4 |
| 1.5 and 14 m | 42.9 | - | 85.7 |
| 4.3 and 14 m | 35.7 | - | 100.0 |
| all antennas | 35.7 | 100.0 | 71.4 |

This analysis permits at least a qualitative estimate on the effectiveness of vertical space diversity. Table IV shows that for installations of this type there is at least a 0.357 probability that 10 db fadeouts occur simultaneously on three vertically spaced antennas. There are substantially more fadeouts on a high antenna while there is

more correlation between fadeouts occuring simultaneously on the two lower antennas.

These figures are operationally important, as a 10 db fadeout necessitates that much margin in available transmitter power for one-way (communications) application. In a radar application, a 10 db fadeout means a 20 db reduction in signal level, as the signal travels both ways. A corresponding increase in transmitter power is necessary.

Although the percentage of total time or total hours during which fadeouts occur is small, it should be kept in mind that such fadeouts are relatively long, and may impair the usefulness of a communications or navigation system for minutes at a time. Fig. 13 shows the cumulative distribution of the durations of 5 db and 10 db fadeouts for all three antenna heights, using all data available for December, 1953. (The previous comparative analysis was restricted to those hours where data were available for all three antennas.) Table V, below, shows the median fadeout duration, and the duration of 10% of all fadeouts, taken from Fig. 13.

TABLE V

Fadeout Durations for December 1953

Cheyenne Mountain-Karval Path, 1046 Mc

| | Duration in Minutes Greater than | | | |
|---|---|---|---|---|
| | Median Fadeout | | 10% of all Fadeouts | |
| Antenna Height, Meters | 5 db | 10 db | 5 db | 10 db |
| 1.5 | 10.6 | 3.5 | 39 | 20.5 |
| 4.3 | 10.4 | 5.7 | 45 | 18.5 |
| 14.0 | 6.1 | 5.0 | 60 | 56.0 |

This table shows that the median fadeout tends to be shorter for the higher antenna, but that a small number of fadeouts observed on the high antenna (10% of the total) tend to be quite long (about one hour). The statement holds approximately for both levels investigated, although the median 10 db fadeout observed on the lowest antenna is relatively short.

Finally, Fig. 14 shows the cumulative distribution of the maximum measured depth of all fadeouts. There does not appear to be any marked distinction between the three antenna heights.

## 3. SOUTHERN CALIFORNIA DATA (NAVY ELECTRONICS LABORATORY)

The profile for this 185 km long path was shown on Fig. 2. The terminals were located on Mt. Wilson and on Point Loma, 1712 and 30 meters above mean sea level, respectively. Data on 138 Mc and 1250 Mc, obtained by the U. S. Navy Electronics Laboratory, were made available to the National Bureau of Standards for analysis. Several months of continuous transmission loss measurements between May, 1950, and February, 1951, were used in this study. Fadeouts were defined and analyzed in the same way as for the Colorado data, namely at several levels (5, 10, and 15 db) below the monthly median of hourly medians of basic transmission loss.

For this path, one of the more interesting results was the existence of a substantial number of fadeouts on a frequency as low as 138 Mc. This is in contrast to the data of Eastern Colorado, where very few pronounced fadeouts were observed on frequencies around 100 and 200 Mc.

The frequency dependence of the fadeouts, and the fadeout dependence on meteorological parameters will be further discussed in connection with the Point Mugu data. Here it should be kept in mind that the climate for Southern California is radically different from the one for continental areas, and may even be termed unique in the sense that a very pronounced stratification of the refractive index structure is almost always present.

The diurnal and seasonal variations of 5 db fadeouts for this path are shown on Figs. 15 and 16. In contrast to the Eastern Colorado path, fadeouts occur here around the clock, with a rather pronounced afternoon maximum on 1250 Mc, and the suggestion of a minimum in mid-morning. The seasonal variations as far as analyzed, are characterized by a minimum in November. Especially striking is the sharp reduction in the number of 1250 Mc fadeouts from October to November, 1950. However, there are not enough data available to make a concise definition of the seasonal trend.

The cumulative distribution of the durations of individual fadeouts is shown on Fig. 17 for both frequencies. It is seen from this figure as well as from Table VI, below, that the fadeouts tend to be longer at the lower frequency. However, the fadeout incidence (number of fadeouts in a given time period) is greater for the higher frequency, as shown on Fig. 16. The distributions have been replotted for both frequencies on Fig. 18 similar to the representation shown on Fig. 12 for the Cheyenne Mountain-Karval path.

Table VI, below, summarizes some of the results of the analysis of the N.E.L. data. No correlation studies between fadeout occurrence on the two frequencies were performed. A comparison of fadeout characteristics for the Colorado and the California paths will be presented in a later section of this paper.

TABLE VI

Fadeout Durations for N.E.L. Path, Southern California

| | Fadeout Durations in Minutes (greater than) | |
|---|---|---|
| | 138 Mc | 1250 Mc |
| for median fadeout | | |
| to 5 db | 6.6 | 2.6 |
| to 10 db | 5.7 | 1.7 |
| to 15 db | 3.9 | 1.1 |
| for 10% of all fadeouts | | |
| to 5 db | 39.1 | 10.0 |
| to 10 db | 37.1 | 7.1 |
| to 15 db | 18.8 | 4.2 |

## 4. SOUTHERN CALIFORNIA DATA (POINT MUGU)

### 4.1 General

The joint propagation study conducted by the Naval Air Missile Test Center, Point Mugu, California, and the National Bureau of Standards was originally designed to compare within-the-horizon and beyond-the-horizon over water paths of approximately the same length. Meteorological data to support the transmission loss measurements were supplied by the U. S. Naval Air Station at Point Mugu. The profiles for the within-the-horizon paths are shown on Fig. 3.

Important results of this program have been reported previously by Barsis and Capps [1957]. Additional data evaluated since are presented here. The following data form the basis for a study of space-wave fadeouts, and their dependence on path and meteorological parameters.

(a) Evaluation of two years radio data on 394 Mc, including correlation of the observed fadeout phenomena with refractive index profile types.

(b) Comparison of fadeout data on the three frequencies (approximately 100, 250, and 400 Mc) for typical winter and summer months.

(c) Comparison of fadeout data for two widely spaced (vertically) receiving sites within the radio horizon.

## 4.2 Classification of Refractive Index Profiles

It will be appropriate to discuss first the evaluation of the meteorological data, and the classification of the refractive index profiles. The data supplied by the Point Mugu Naval Air Station included pseudo-adiabatic charts from radiosonde ascents at San Nicolas Island and at Point Mugu, and surface observations of temperature, barometric pressure, and relative humidity. From these data the refractivity as a function of height was computed and plotted in the form of curves of a modified refractive index as a function of height defined by Bean, et al [1959b]. Values of the surface refractivity were determined as well.

The modified refractive index A(h) at a height h above the surface is given by

$$A(h) = N(h) + 313\,[1 - \exp(-0.144h)] \qquad (2)$$

where N(h) is the refractivity at the height h above the surface (in kilometers). The constants used in this formula are derived from observations within the United States, as explained by Bean, et al [1959b]. The "standard exponential atmosphere" would be a vertical straight line, if plotted in terms of A-units.

This representation has been used in order to make the distinction between various types of refractive index profiles more evident. Previous radio meteorological studies have shown that within the Pacific Coast region refractive index profiles characterized by a constant gradient are much less frequent than the occurrence of either elevated or ground-based layers. Consequently, the calculation of transmission loss as a function of refractive index gradient is not often expected to give results comparable to the measured values. Actual transmission loss calculations taking into account existing layers may be performed by analytical or by ray-tracing methods as suggested by Doherty [1952]. However, the procedure tends to become quite involved. It has been found more convenient to investigate the transmission loss and other characteristics of the received field empirically as a function of various properties of the refractive index profiles. The first step in an analysis of this kind is to define characteristic parameters of the refractive index profiles, and to classify the profiles into easily recognizable types.

Fig. 19 illustrates the five basic profile types used, plotted as A-curves. Classification is made in accordance with the height above ground $h_1$ of the base of the lowest super-refractive layer, the thickness $h_2$ of the layer, the refractive index gradient $\Delta N_1$ existing below the layer, and the refractive index gradient $\Delta N_2$ within the layer. A super-refractive layer is somewhat arbitrarily defined to exist if its refractive index gradient is greater than 60 N-units per kilometer.* The classifications shown on Fig. 19 are tabulated and explained below:

* In this and the following analyses the expressions "greater than," "less than," "in excess of," ect., are based on the use of absolute values of refractive index gradients. It is understood that refractivity generally decreases with height, and that the refractive index gradient is almost always negative.

| Type of Profile | | |
|---|---|---|
| Linear | L | Refractive index gradient less than 60 N-units per kilometer for the entire profile. |
| High Elevated Layer | HE | Base of layer higher than one kilometer above the surface with $\Delta N_1$ less than, and $\Delta N_2$ in excess of 60 N-units per kilometer. |
| Medium Elevated Layer | ME | Like HE, but base of layer between 0.5 kilometers and 1.0 kilometer above the surface. |
| Low Elevated Layer | LE | Like HE, but base of layer less than 0.5 kilometers above the surface. |
| Ground Based Layer | GB | Surface based layer, with $\Delta N_2$ in excess of 60 N-units per kilometer. |

As an illustration of the effect of the refractive index profiles on the character of the received signal, consider Fig. 20, which contains two chart samples of the Laguna Peak record representing the within-the-horizon path. The upper record, taken at a time when a linear refractive index was observed at Pt. Mugu, shows a virtually constant signal over a period of several hours. The lower record corresponds to a time when ground-based layers were observed at Pt. Mugu, and shows very substantial space-wave fadeouts.

Table VII, below, shows the relative frequency of occurrence of the various profile types at both sounding locations during the period November 1955 to October 1957. It is not possible to distinguish between "ground-based" (GB) and "low elevated" (LE) layers for profiles observed at San Nicolas Island, as the radiosonde measurements were conducted from an airstrip located about 170 meters above sea level, but close enough to the coast so that sea level is the actual reference.

TABLE VII

Occurrence of Various Profile Types

November 1955 to October 1957

| Profile Type & Total Number Observed | Number of Times Observed | | Percentage of Total Observations | |
|---|---|---|---|---|
| | Pt. Mugu | San Nicolas Island | Pt. Mugu | San Nicolas Island |
| L - 93 | 66 | 27 | 21.9 | 7.5 |
| HE - 55 | 28 | 27 | 9.3 | 7.5 |
| ME - 117 | 62 | 55 | 20.6 | 15.3 |
| LE } - 395 | 52 | } 250 | 17.3 | } 69.7 |
| GB } | 93 | | 30.9 | |
| Totals: 660 | 301 | 359 | | |

It is quite evident that profiles characterized by layers below 1000 meters predominate. More than half of all observations indicate layers below the 500-meter level. Both path terminals for the propagation studies were located below this elevation. The effect of the layer height on the propagation characteristics will be discussed below. In this study, profiles observed at both sounding locations will be used. Of all observations there were only 96 radiosonde ascents taken approximately simultaneously at both locations (within about one and one-half hours). 62 profiles out of these 96, or somewhat more than one-half, showed the same profile type in accordance with the classification used. Although this conclusion does not fully support the assumption of complete equivalence of the profiles obtained at the two locations, it does not preclude the use of all profiles regardless of their origin for further analysis.

## 4.3 Dependence of Fadeout Characteristics on Profile Types

For this study, the 394 Mc data for the path San Nicolas Island - Laguna Peak Summit were used (see Fig. 3), covering the period November 1955 to October 1957. Within this period approximately 14,000 hours of good data were obtained. However, in the study of fadeout dependence on refractive index profile types, only those data were used which fell within the three-hour period centered on the time of the radiosonde ascent. Soundings were usually taken around 8 a.m. local time; in some instances additional soundings were taken between noon and 4 p.m.

In this analysis a fadeout was defined as a reduction in signal level to at least five or ten decibels below the monthly median lasting at least one minute. The terms "fadeout incidence" and "fadeout time" are used. Fadeout incidence is the number of times fadeouts are observed concurrently with a specific type of refractive index profile, expressed in percent. Fadeout time is the total time the signal remained at least 5 or 10 db below the monthly median. It is also expressed in percent relative to the three-hour period centered on the radiosonde ascent. As an example, 32.3% 5 db fadeout incidence for linear profiles means that out of the total number of linear refractive index profiles observed, 32.3% have one or more prolonged 5 db space-wave fadeouts associated with them which occurred within the three-hour period centered on the meteorological observation. As an example of 5 db fadeout time, 19.9% for ground-based layers means that during 19.9% of three hour time interval centered on the meteorological observation (35.8 minutes) the signal remained at least 5 db below the monthly median. Results of the analysis are given in Table VIII, below.

TABLE VIII

Fadeout Characteristics Versus Refractive Index Profile Types
San Nicolas Island to Laguna Peak (Summit)
394 Mc, November 1955 to October 1957

| Profile Type | Total Number of Observed Profiles | Percentage of Fadeout Incidence | | Percentage of Fadeout Time | |
|---|---|---|---|---|---|
| | | 5 db | 10 db | 5 db | 10 db |
| Linear (L) | 93 | 32.3 | 18.3 | 10.7 | 2.7 |
| High Elevated Layer (HE) | 55 | 16.4 | 7.3 | 5.3 | 1.4 |
| Medium Elevated Layer (ME) | 117 | 30.1 | 18.8 | 6.9 | 2.3 |
| Low Elevated Layer (LE) | 302 | 70.2 | 50.0 | 20.9 | 7.7 |
| Ground-Based Layer (GB) | 93 | 66.7 | 51.6 | 19.9 | 8.6 |
| L + HE | 148 | 26.4 | 14.2 | 8.7 | 2.4 |
| ME + LE + GB | 512 | 60.6 | 43.2 | 17.5 | 7.0 |
| L + HE + ME | 265 | 28.3 | 16.2 | 7.9 | 2.4 |
| LE + GB | 395 | 69.4 | 50.4 | 20.6 | 8.3 |
| All Profiles | 660 | 52.9 | 36.7 | 15.5 | 5.9 |

It is seen that fadeout incidence and fadeout time are both functions of the profile type. Substantially more fadeouts and more fadeout time were observed at the 5 and the 10 db level for the low elevated and ground-based layers than for the other types. The various combinations of profile types used in Table VIII show that the effect of medium-height elevated layers (between 500 and 1000 meters above the surface) may be included in either of the two groups (L and HE, or LE and GB) without any substantial change. The figures for the combination of all

profile types show that for this path the overall fadeout incidence is 36.7%, and the overall fadeout percentage is 5.9%, both for the operationally important 10 db fadeouts.

Fig. 21 shows the dependence of fadeout time, as defined above for 5 db fadeouts, on the refractive index profile parameters $h_1$, $h_1 + h_2$, and $\Delta N_2$: $h_1$ is the elevation of the base of the layer above the surface (in this case, mean sea level), $h_1 + h_2$ is the elevation of the top of the layer with $h_2$ indicating the thickness of the layer, and $\Delta N_2$ the refractive index gradient within the layer. The same data were used in this study, as before (for Table VIII), except that only 5 db fadeouts were considered. The graphs were obtained by an averaging procedure described below, resulting in mean percentage fadeout time, and the standard deviations of the individual mean values indicated by the vertical "wings" about the points shown.

The abscissa scale on Fig. 21(a) represents the height $h_1$ of the layer base. For the purpose of averaging, the heights $h_1$ were divided into intervals of 0.2 kilometers up to a value of 1.4 kilometers. Values of percentage fadeout time corresponding to each height interval were averaged, and the resulting mean values plotted on Fig. 21(a) as ordinates at the abscissa values corresponding to the mean height within the interval. As an example, the point plotted at $h_1 = 0.49$ kilometers, and 9.6% fadeout time is the mean value of percentage fadeout time observed for all hours when the layer height, $h_1$, was between 0.4 and 0.6 kilometers. To illustrate some special cases, the point plotted at $h_1 = 0$ corresponds to the mean value of percent fadeout time for all occurrences of a ground-based layer. The value plotted at $h_1 = 1.82$ kilometers represents the average for all layer heights in excess of 1.4 kilometers, and the value corresponding to linear profiles is plotted at the far right of the graph, as it may be considered a limiting value with $h_1$ approaching infinity.

In a similar way the percentage fadeout time has been plotted versus the elevation of the top of the layer ($h_1 + h_2$) on Fig. 21(b). Here the linear profile may be considered a limiting case if $h_1 + h_2$ approaches zero as well as infinity. On this graph the subdivision of the heights into 0.2 kilometer intervals was carried on to 2.0 kilometers, with all greater heights lumped together to give a single average value.

On Fig. 21(c) the abscissa scale represents the refractive index gradient $\Delta N_2$ within the layer. This scale was divided into intervals of 20 N-units for the averaging process. This graph does not include values corresponding to linear profiles, because by definition of the profile types a linear profile does not have a value of $\Delta N_2$ associated with it.

On all graphs the vertical wings about each mean represent an estimate of the standard deviation of the mean, which is actually the standard deviation of the individual means about their overall mean.* The extent of the wings relative to the variations of the mean values themselves serve as a rough estimate of the existence of a trend in the data.

The graphs of Fig. 21 provide additional information on the dependence of fadeout time on layer characteristics, whereas the results shown in Table VIII apply to a more general classification of the layers. Fig. 21(a) shows quite clearly that the percentage fadeout time is greatest for ground-based and very low layers (below 200 meters above the surface). The dependence on the height of the top of the layer shown in Fig. 21(b) indicates maximum fadeout time for heights $h_1 + h_2$ below

---

* The standard deviation of the mean, $s_m$, is obtained from the standard deviation s of the individual values by dividing by $\sqrt{n}$, where n is the number of values averaged. $s_m$ therefore includes the effect of the number of measurements in any particular group.

800 meters. Both terminals are well below this height, suggesting that a well-defined discontinuity in the refractive index profile structure favors the occurrence of fadeouts, if the ray paths penetrate the discontinuity. The second maximum on Fig. 21(b) appears to be less significant due to the wide spread of the data.

Fadeout time dependence on the refractive index gradient $\Delta N_2$ within the layer is not significant, as shown by Fig. 21(c).

Summarizing the results of this particular study, it appears that fadeout incidence and fadeout time are strongly dependent on the existence of refractive index profile discontinuities, and are a function of layer height above the surface. Layers which start at elevations substantially above the path terminals do not seem to produce as many fadeouts as the ones which are at elevations comparable to the height of the ray paths.

## 4.4 Dependence of Fadeout Characteristics on Carrier Frequency and Grazing Angle

In addition to the 394 Mc data obtained since November, 1955, on the path San Nicolas Island - Laguna Peak Summit, some data are available on other frequencies during two short periods. From November, 1957, until January, 1958, transmissions on 100 Mc, 244 Mc, and the original 394 Mc frequency were recorded over the same path. From April to the beginning of August, 1959, 98.3, 249, and 394 Mc were used. Furthermore, an additional receiving site, called the "Van" location was established on Laguna Peak at an elevation of 254 meters above mean sea level, which is still within the radio horizon of the transmitting antenna location. This site was also in use between April and August of 1959. A 394 Mc receiver was installed there, permitting

comparison of the signal characteristics at the same frequency, but for different grazing angles (2.0 and 3.6 milliradians, respectively). For all frequencies, vertical polarization with corner-reflector antennas were used.

Very little meteorological data could be obtained for these two recording periods, so that the evaluation of the data will be restricted to studies of the carrier frequency and antenna height (or grazing angle) dependence of the fadeouts without any correlation with meteorological data.

Fadeout incidence (here the number of fadeouts in a 90-day period) for the winter and summer measurement period mentioned above are shown on Fig. 22 as a function of carrier frequency. For this study, fadeouts have been defined relative to the hourly median signal level as well as relative to the median of all hourly medians within a month as previously used. The graphs show points for 10 and 20 db fadeouts at the three frequencies, arbitrarily connected by straight lines. Data for the "Van" location have also been included. It is seen that there is a strong frequency dependence, especially for the winter period. The grazing angle dependence is more pronounced for the fadeouts measured relative to the monthly medians, as the "Van" points are more separated from the solid line which denotes the "Summit" data. It should also be noted that there are more than one hundred 20 db fadeouts in a 90-day summer period on 394 Mc, which would correspond to more than one such fadeout per day if evenly distributed. The operational importance of this frequency of occurrence cannot be overemphasized.

Examples of the diurnal variations of the space-wave fadeouts observed on the three frequencies are shown on Figs. 23 and 24. Here the summer data are used (April - August, 1960), and the data are

separated into four time blocks as defined by Norton, et al [1955], corresponding to early-morning, mid-morning, afternoon, and evening hours. On Fig. 23, the ordinate values show the number of fadeouts per hour, and the data are grouped by frequency (for both, the "Van" and the "Summit" locations), time blocks, and depth of fadeouts relative to the hourly medians. It is seen that there are generally more fadeouts at the "Summit" location (which corresponds to a larger grazing angle) than at the "Van." A slight diurnal trend is discernible with the fadeout incidence greatest for the afternoon hours, except for the 5 db fadeouts, on 394 Mc which occur most frequently in the early evening hours. A similar trend is noted for the 249 Mc and the 100 Mc data, although there may not be enough of the latter to draw any valid conclusions.

On Fig. 24, the ordinate is in percent fadeout time, and only 10 db fadeouts below the monthly medians are used. Percent fadeout time is then the percentage of total time the signal remained at least 10 db below the monthly median. This percentage is also higher for the "Summit" data than for the "Van" data. As there are also more fadeouts at the "Summit" (see Fig. 22), the duration of the individual fadeouts may be expected to be approximately equal at both locations. This will be further discussed below.

Fig. 24 also shows that fadeout times on 394 and 98.3 Mc are comparable. Referring again to Fig. 22, it is seen that there are less fadeouts on 98.3 Mc than on 394 Mc. This leads to the conclusion that the individual fadeouts tend to be longer on the lower frequency. A comparison of the N.E.L. data on 138 Mc and 1250 Mc lead to the same results (see Table VI in Section 3, above).

The diurnal trend of the percentage fadeout time is similar to the trend in the number of fadeouts shown on Fig. 23. This also agrees with the results for the N.E.L. path (see Fig. 15).

Some of the basic data used to prepare Figs. 22 and 24 are shown in Table IX below. The table contains fadeout data with reference to the monthly medians. Data with respect to the hourly medians were shown on Fig. 23.

TABLE IX

Fadeout Statistics for San Nicolas Island - Laguna Peak Path, April - July, 1959, 10 db Fadeouts Relative to Monthly Median Level

| Frequency Mc | Total No. of Hours of Data | Number of Fadeouts Observed | | Percentage Fadeout Time | Average Fadeout Duration, Minutes |
|---|---|---|---|---|---|
| | | Total | Normalized to 90 Days | | |
| 394 (Summit) | 2648 | 957 | 781 | 4.07 | 6.8 |
| 394 (Van) | 1751 | 408 | 503 | 2.80 | 7.2 |
| 249 | 2288 | 256 | 242 | 3.18 | 17.0 |
| 98.3 | 1015 | 108 | 230 | 4.30 | 24.2 |

An example of a more complete analysis of fadeout duration is shown on Fig. 25 which depicts cumulative distributions of the duration of 10 db fadeouts for both periods relative to monthly and hourly medians. Here the minimum measured duration of fadeouts relative to the hourly median was approximately 0.4 minutes. The curves are labelled with the total number of the 10 db fadeouts observed in each case, and are coded to denote the different frequencies and paths. As an example, the dotted curve on the lower left-hand graph for 249 Mc shows that for the summer period 50% of all fadeouts observed on this frequency to at least 10 db below the monthly median had a duration of 7 minutes, or longer; 10% of these fadeouts were as long as 27 minutes, and 90% of them, 1.8 minutes.

Comparing the 50% (median) values from the lower left-hand graph with the corresponding average fadeout duration values for the same period from Table IX it appears that the median fadeout duration is substantially less than the average fadeout duration. This may be explained by the fact that there are many more relatively short fadeouts than very long ones, and in calculations of averages the long fadeouts have more weight. The appearance of Fig. 25 suggests a log-normal distribution of fadeout durations, as they are plotted using a logarithmic ordinate scale.

Comparison of the four graphs of Fig. 25 shows additional results which are summarized in Table X below.

TABLE X

Median Fadeout Duration at the 10 db Level

| Nominal Frequency | Fadeout Duration in Minutes | | | |
|---|---|---|---|---|
| | Relative to Monthly Median | | Relative to Hourly Median | |
| | Winter | Summer | Winter | Summer |
| 400 Mc (Summit) | 5.4 | 3.5 | 2.2 | 1.70 |
| 400 Mc (Van) | No Data | 3.4 | No Data | 1.60 |
| 250 Mc | 6.6 | 7.0 | 1.80 | 1.95 |
| 100 Mc | 14.0 | 9.1 | 9.0 | 3.0 |

It is seen that:

(a) Fadeouts are longer and more frequent if measured relative to the monthly transmission loss medians than relative to the hourly transmission loss medians. This results from the substantial variations in the hourly median levels over the period of one month.

(b) Fadeouts are generally shorter, but more frequent in summer.

(c) The frequency dependence of fadeout duration is more pronounced if fadeouts are measured relative to the monthly median than if measured relative to the hourly median. (The 100 Mc curve on the upper right-hand graph of Fig. 10 is based on only three data points, and therefore may not be reliable.) On the basis of Table X, one may also conclude that there is little frequency dependence of fadeout duration measured relative to the hourly median in the 250-400 Mc range, whereas the frequency dependence in this range is much more apparent if fadeout durations are measured relative to the monthly medians.

(d) The curves for the "Summit" and the "Van" locations, both for 394 Mc, are almost coincident. It is concluded that no effects of the grazing angle on fadeout duration has been found in the data analyzed here.

Distribution curves of fadeout durations for 394 Mc have been replotted on Fig. 26 in the same form as Figs. 12 and 18, in order to facilitate their application to reliability studies of communication circuits. On Fig. 26 the fadeout duration distributions are compared for the "Summit" and the "Van" locations, with the fadeouts measured relative to the hourly median. The median fadeouts (the curves labelled "50%") taken from Fig. 26 have durations at the various levels as shown on Table XI, below. The values at the 10 db level do not agree exactly with the values shown previously in Table X, because the curves of Fig. 26 have been smoothed.

TABLE XI

Duration of Median Fadeouts at Various Levels
Relative to the Hourly Median, 394 Mc
San Nicolas Island - Laguna Peak Path

| Level, db | Duration, Minutes | |
|---|---|---|
| | Summit | Van |
| 5 | 3.5 | 3.5 |
| 10 | 2.0 | 1.6 |
| 15 | 1.4 | 0.96 |
| 20 | 1.06 | 0.65 |
| 25 | 0.87 | 0.49 |
| 30 | 0.75 | 0.38 |
| 35 | 0.66 | 0.31 |

Some of the larger db values were obtained by extrapolation of the curves. The curves on Fig. 26 and the data in Table XI show that the fadeout durations tend to be shorter for the Van location, which corresponds to a smaller grazing angle. This trend was not apparent in the average fadeout duration values listed in Table IX.

## 5. FADEOUTS ON A KNIFE-EDGE DIFFRACTION PATH

During the past year, transmission loss measurements were made over a 223 km path in Colorado, using continuous-wave signals on 751 Mc. Fig. 4 shows the path profile. The top of Pikes Peak, 4292 meters above mean sea level, forms the diffracting knife-edge. The transmitting installation is located near Beulah (southwest of Pueblo), and the receiving installation is on Table Mesa, north of Boulder. A complete description of the equipment used and the

measurements performed are contained in a separate paper [Barsis and Kirby, 1961]. The data discussed here are concerned with prolonged space-wave fadeouts observed on this path on two receiving antennas, spaced vertically by approximately 20 wavelengths.

Although this path is not "optical" (terminals within each other's radio horizon), the fading characteristics may be compared with the ones previously described, because the received field may be considered as the vector sum of up to four rays, each of which is modified in magnitude and phase by the diffracting knife edge [Dickson, et al, 1953]. Fig. 27 shows a typical sample of field strength records obtained simultaneously from the two receiving antennas. The fadeouts in this case appear to be extremely well correlated, just as in the case of the Cheyenne Mountain - Karval path (Fig. 6). Here, too, the small, superimposed more rapid signal variations have not been considered in the analysis. Fig. 27 suggests that fadeout phenomena on this obstacle gain path are similar to the ones observed on the within-the-horizon paths, and that vertical space diversity would be of little use due to the apparent correlation of the fadeouts observed on the two antennas.

An analysis of fadeouts was made of the data recorded using the two spaced receiving antennas. The lower of the two was a 3 meter (10 ft) parabolic reflector, 8 meters above ground, and the upper one a corner reflector 15 meters above ground.* The transmitting antenna was a 4.5 meter (14 ft) parabolic reflector mounted 7 meters above ground level. Horizontal polarization was used for all tests. Continuous recordings were available during 8 five-day periods between May and September, 1960.

* During two of the five-day recording periods (in June), the corner reflector was at an elevation of 23 meters above ground. No material difference in the characteristics of the fadeouts at the two elevations was found.

The diurnal trend in the number of fadeouts observed at various levels below the hourly median is shown on Fig. 28. In order to provide a better comparison of fadeout incidence for the various time blocks, the number of fadeouts per hour is shown for each time block. Several facts stand out in a study of this graph. First, the 5 db fadeouts are much more frequent than expected from a comparison with the other levels, especially for the higher antenna (the corner reflector). Then, the diurnal trend for the 5 db fadeouts is different from the others, showing a maximum for Time Blocks 4 or 5 (0600 to 1300 and 1300 to 1800 local time). For all other levels, maximum fadeout incidence is observed during Time Block 7, the early morning hours (midnight to 0600 local time). It is also noted that the minimum fadeout incidence is less pronounced for the 5 db level than for the other levels. This minimum occurs in Time Block 5, the afternoon hours (1300 to 1800 local time). There are also substantially more 5 db fadeouts on the higher antenna during daylight hours (Time Blocks 4 and 5).

All this suggests the existence of two separate propagation mechanisms, with one producing only 5 db fadeouts, and the other one responsible for the deeper fadeouts. The latter mechanism might be similar to the one responsible for the fadeouts on the within-the-horizon paths.

The cumulative distributions of fadeout durations for this path are shown on Fig. 29 for both antennas. Here, fadeout durations as short as 0.1 minutes could be measured. It is quite apparent here, especially for the corner reflector, that the 5 db fadeouts have different characteristics than the others. The cross-over of the 5 db curve implies again that there are many of these 5 db fadeouts which do not extend to deeper levels, and might be due to a different phenomenon.

Table XII, below, is a tabulation of median fadeout durations taken from Fig. 29.

TABLE XII

Median Fadeout Durations at Levels Below the Hourly Median
Colorado Obstacle Gain Path, 751 Mc, Summer 1960

| Level, db below Hourly Median | Median Fadeout Duration, Minutes | |
|---|---|---|
| | Corner Reflector | 3 Meter Dish |
| 5 | 0.72 | 0.66 |
| 10 | 0.81 | 0.62 |
| 15 | 0.66 | 0.44 |
| 20 | 0.50 | 0.27 |

It is seen that the median fadeout at all levels is longer on the corner reflector antenna. The different behavior of the 5 db fadeouts is again apparent by their median duration, which is actually less for the corner reflector than the median duration of the 10 db fadeout. For the 3 meter dish the median durations at these two levels are comparable.

The data from Fig. 29 have been replotted on Fig. 30 in order to show the level distributions for individual fadeouts. This is the same type of presentation which was used on Figs. 12, 18, and 25 for the other paths. Due to the possibility of a different mechanism being responsible for 5 db fadeouts, the curves were based on the 10, 15, 20, and 25 db levels read from Fig. 29, and extrapolated to lower and higher levels. The curves shown on Fig. 30 were smoothed by the "firm-grip-on-the-pencil" method, just as the equivalent ones for the other paths. These types of curves, as mentioned before, will be

used as a basis for system performance or circuit reliability estimates in a companion paper.

The effectiveness of vertical space diversity for this path may also be evaluated by the number of fadeouts occurring simultaneously on both antennas as a percentage of the total number of observed fadeouts. This is the same evaluation as was done for the three vertically spaced antennas at Karval (see Section 2.3), except that the fadeouts were measured with respect to the hourly median over the Pikes Peak obstacle gain path. The results are given in Table XIII, below, using 5 db and 10 db fadeouts. For this study summer data with the corner reflector antenna at the 23 meter elevation were excluded, so that only those data were used for which the antenna separation was 7 meters (17.5 wavelength at 751 Mc). Fadeouts were classified as simultaneous when any portion of them coincided in time.

TABLE XIII

Statistics of Simultaneous Fadeouts, Pikes Peak Obstacle Gain Path, Summer 1960, 751 Mc

| | Receiving Antenna | |
|---|---|---|
| | 3-Meter Dish at 8 Meters | Corner Reflector at 15 Meters |
| 5 db Fadeouts | | |
| Total Number Observed | 464 | 681 |
| Number of Simultaneous Fadeouts | 175 | 175 |
| Percentage of Simultaneous Fadeouts | 37.7% | 25.7% |
| 10 db Fadeouts | | |
| Total Number Observed | 120 | 151 |
| Number of Simultaneous Fadeouts | 32 | 32 |
| Percentage of Simultaneous Fadeouts | 30.0% | 21.2% |

The total number of fadeouts shown on Table XIII is different from the corresponding data on Fig. 29 because of the exclusion of the two-week period when the corner reflector antenna was at a higher elevation. Comparison with the Karval data in Section 2.3 shows again a greater number of fadeouts for the higher antenna. The percentage of simultaneous fadeouts appears to be smaller: this might be due to the fact that it was not possible to synchronize the time scales exactly when the recording charts were analyzed. As a great number of the fadeouts were shorter than one minute, a small shift in the time scale may change the apparent relative time of occurrence of some short fadeouts. Even so, the results given in Table XIII show that there is a probability of 0.212 that 10 db fadeouts (relative to the hourly median of transmission loss) occur simultaneously on the two spaced antennas. This may be compared with the 0.357 probability from Table IV, as obtained for the Cheyenne Mountain - Karval path.

If the two-week period mentioned is included in the studies, the fadeout percentages shown in Table XIII decrease slightly. It is difficult to say whether this constitutes a true effect of antenna height, or is caused by the inclusion of an additional time period; height gain effects can be properly evaluated only when simultaneous measurements are available. The two weeks of data in question have been included in the study of distributions of fadeout durations without any significant change in the results, as mentioned above.

## 6. COMPARISON OF THE RESULTS FOR THE VARIOUS PATHS AND CONCLUSIONS

The results discussed in Sections 2 through 5 above permit various comparative evaluations of fadeout characteristics. The climatic effects may be studied by comparing results obtained in Colorado with

those obtained at the Pacific Coast. Frequency effects are available from the Pacific Coast measurements, and space diversity studies from the Colorado measurements. A detailed study of the effect of refractivity profiles on fadeout characteristics was only performed for the Point Mugu data, and has been discussed in Section 4.3, above.

General climatic effects are summarized in the following table by comparing diurnal and seasonal variations of the fadeout characteristics.

TABLE XIV

Comparison of Diurnal and Annual Variations of Fadeout Characteristics

| | Eastern Colorado | | Pacific Coast | |
|---|---|---|---|---|
| | Karval Path | Obstacle Gain Path | Mt. Wilson Path | Point Mugu Path |
| Seasonal Trend of Fadeout Incidence | Summer Maximum | Not Investigated | Not Pronounced | Not Pronounced |
| Diurnal Trend of Fadeout Incidence | Nighttime Maximum | Morning Maximum | Afternoon Minimum | Afternoon Minimum |
| Median Fadeout Duration for 1000 Mc Range, 10 db Fadeouts | 5.0 Minutes | * | 5.7 Minutes | - |

* Not investigated for fadeouts relative to the monthly median.

Outstanding effects are the very definite lack of fadeouts during daytime hours for the Karval path, and the absence of any pronounced seasonal variations for Pacific Coast data, as far as investigated. It is also noted that maximum fadeout incidence for the Karval path is at

night, whereas it is shifted to the morning hours for the Pikes Peak obstacle gain path. Median fadeout durations at 1000 Mc at the 10 db level relative to the monthly median are comparable for both areas.

Diurnal and seasonal trends in the occurrence of fadeouts similar to the ones observed at Karval were reported from measurements at 1300 Mc over a 82 km overland path within the radio horizon, located in East Germany [Kuehn, 1957]. Despite the difference in the general climatology, the low-level modifications of the refractive index structure which are most likely to produce fadeouts appear to have similar diurnal and seasonal trends in both regions. Knehn's data, like the ones obtained at Karval, show a minimum occurrence of fadeouts around the noon hour, strong maxima at night, and also substantially more fadeouts during the summer months.

Almost no fadeouts at all were observed on lower frequencies over the Colorado Paths. The frequencies used concurrently with 1046 Mc were 100 and 192.8 Mc for Cheyenne Mountain - Karval, and 100 Mc for the Pikes Peak obstacle gain path. In contrast thereto, a sufficient number of fadeouts for evaluation was observed on 138 Mc for the Mt. Wilson path, and on 100 Mc for the Point Mugu path. This again may be an indication of the radical climatic differences between a continental and a maritime area.

The effects of vertical space diversity have been discussed for both Colorado paths in Sections 2.3 and 5. It appears that fadeouts are reasonably well correlated at antenna spacings which might be practical for diversity arrangements, and thus impair the effectiveness of vertical space diversity for line-of-sight paths as well as the obstacle gain paths. It already has been mentioned that during two of the recording periods in June the vertical spacing was increased to 15 meters between the two antennas. No significant change in the apparent signal characteristics was observed.

The two antennas on Laguna Peak are too far apart to consider such an arrangement a practical diversity system. The experiment was designed in this case to study the effect of the grazing angle on fadeouts. Although results are not very pronounced, there is a tendency for more fadeouts on the summit of Laguna Peak, representing a greater elevation and a greater grazing angle (see Fig. 22). This result is also somewhat supported by the Colorado height-gain studies, where substantially more fadeouts were observed at the higher antennas. (See Table II in Section 2.3 and Table XIII in Section 5.)

In conclusion, it is recognized that space-wave fadeouts constitute an important phenomenon in line-of-sight or related propagation characteristics, especially on frequencies above 400 Mc. The phenomenon is observed regardless of climatic conditions, although the structure of the refractive index profile affects its frequency of occurrence. Space-wave fadeouts have to be taken into account in the design of communication systems, because of the relatively long and large drops in signal level. The studies performed so far show that vertical space diversity is not effective in compensating for all fadeouts because of the observed degree of correlation. Experiments on correlation using horizontally spaced antennas or frequency diversity are yet to be performed.

Fadeout statistics as developed in this paper will be used in a companion paper to estimate the performance of communication circuits over paths of this nature. The analysis will be based primarily on fadeout incidence and the distributions of fadeout durations as shown on Figs. 12, 18, 26, and 30.

## 7. ACKNOWLEDGEMENTS

In dealing with an extensive measurement program of this type it is not possible to acknowledge the contributions of individuals. Data collection and evaluation was performed by the Cheyenne Mountain Field Station (partially with the support of the Air Navigation Development Board), the Tropospheric Measurement Section, and the Propagation-Terrain Effects Section of the National Bureau of Standards. We also wish to acknowledge the assistance of the Navy Electronics Laboratory, San Diego, California, and of the Naval Air Missile Test Center, Point Mugu, California, in obtaining data, supplying equipment, and doing analysis work.

The authors wish to thank Messrs. B. R. Bean and R. S. Kirby for their review and suggestions. Drafting work was done by J. C. Harman and his group, and the manuscript was typed by Mrs. D. J. Hunt.

## 8. REFERENCES

Barsis, A. P., J. W. Herbstreit, and K. O. Hornberg, Cheyenne Mountain tropospheric propagation experiments, National Bureau of Standards Circular 554 (Jan. 1955).

Barsis, A. P., and F. M. Capps, Effect of super-refractive layers on tropospheric signal characteristics in the Pacific coast region, IRE 1957 WESCON Convention Record, Part 1, 116-133 (1957).

Barsis, A. P., and R. S. Kirby, VHF and UHF signal characteristics observed on a long knife-edge diffraction path, paper to be submitted for inclusion in the 1961 IRE International Convention Record.

Bean, B. R., Prolonged space-wave fadeouts at 1046 Mc observed in Cheyenne Mountain propagation program, Proc. IRE 42, No. 5, 848-853 (May 1954).

Bean, B. R., L. P. Riggs, and J. D. Horn, Synoptic study of the vertical distribution of the radio refractive index, J. Research NBS 63D, (Radio Prop.), No. 2, 249-254 (Sept.-Oct. 1959).

Bean, B. R., and G. D. Thayer, Central Radio Propagation Laboratory exponential reference atmosphere, J. Research NBS 63D, (Radio Prop.), No. 3, 315-317 (Nov.-Dec. 1959).

Doherty, L. H., Geometrical optics and the field at a caustic with application to radio wave propagation between aircraft, Cornell University School of Electrical Engineering Research Report EE 138 (Sept. 1952).

Dickson, F. H., J. J. Egli, J. W. Herbstreit, and G. S. Wickizer, Large reductions of VHF transmission loss and fading by the presence of a mountain obstacle in beyond-line-of-sight paths, Proc. IRE 41, No. 8, 967-969 (Aug. 1953). A discussion of this paper is given by J. H. Crysdale in Proc. IRE 43, No. 5, 627 (May 1955).

Kuehn, U., Ein Beitrag zur Kentniss der Ausbreitungsbedingungen bei 1.3 GHz nach Messungen an einer Uebertragungsstrecke mit optischer Sicht, Technische Mitteilungen (B.R.F.) 1, No. 1, 4-10 (Oct. 1957), Berlin - Adlershof (East Germany).

Norton, K. A., P. L. Rice, and L. E. Vogler, The use of angular distance in estimating transmission loss and fading range for propagation through a turbulent atmosphere over irregular terrain, Proc. IRE 43, No. 10, 1488-1526 (Oct. 1955).

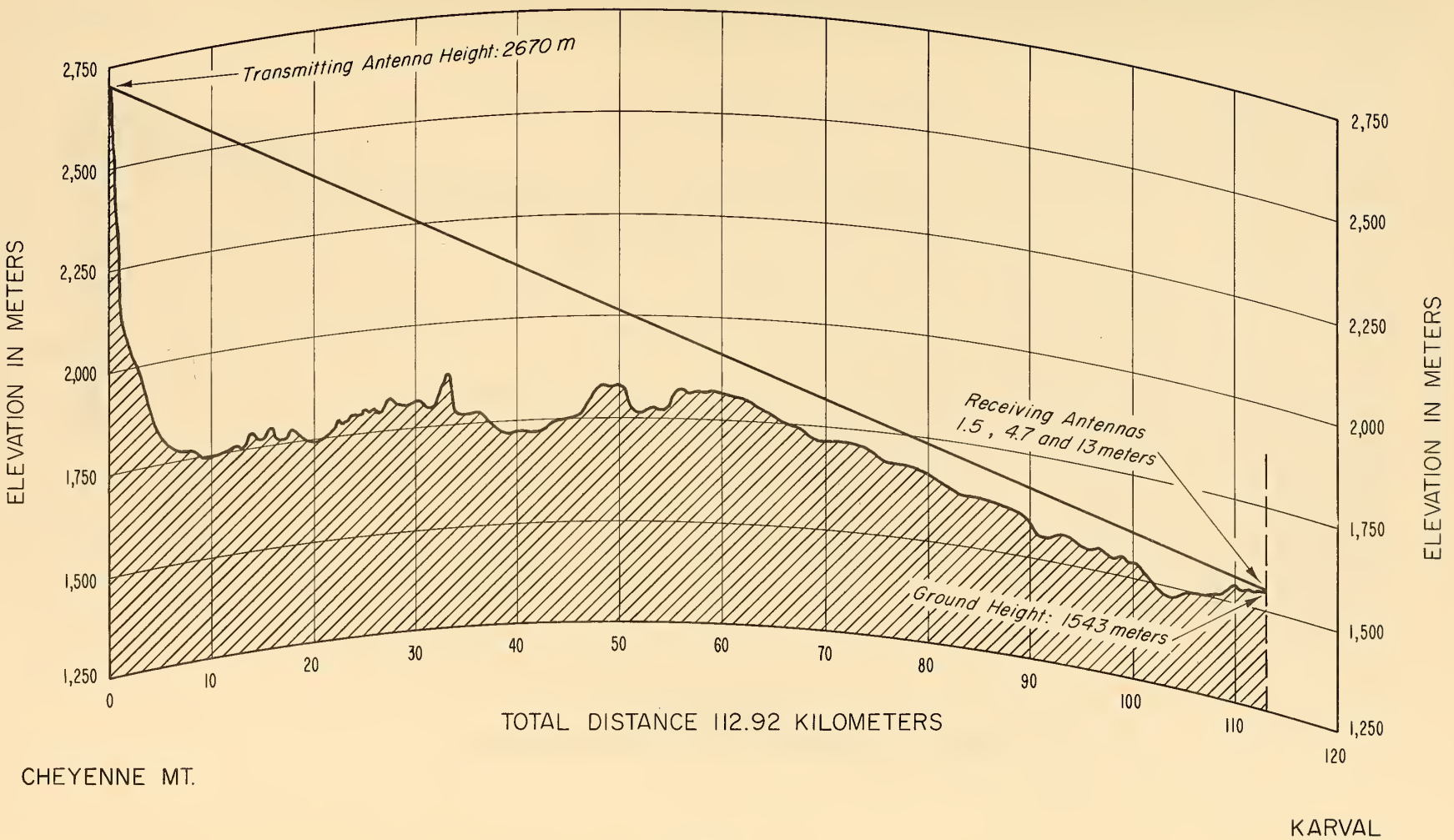
TERRAIN PROFILE CHEYENNE MT. (SUMMIT) – KARVAL
( COLORADO)
Transmitting Antenna Height: 2670 m
Receiving Antennas
1.5 , 4.7 and 13 meters
Ground Height: 1543 meters
ELEVATION IN METERS
2,750
2,500
2,250
2,000
1,750
1,500
1,250
0
10
20
30
40
50
60
70
80
90
100
110
120
TOTAL DISTANCE 112.92 KILOMETERS
CHEYENNE MT.
KARVAL

Figure 1

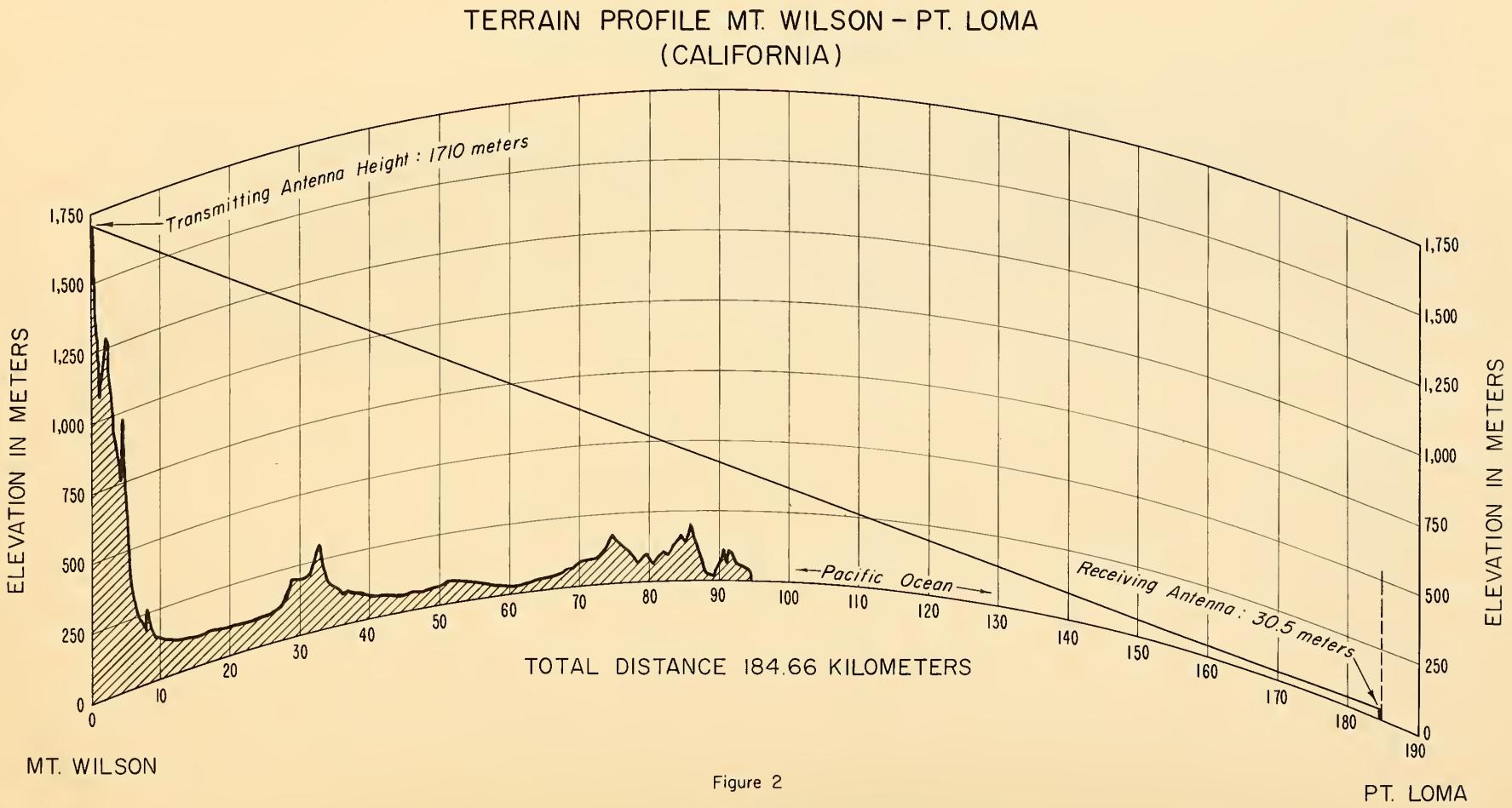
TERRAIN PROFILE MT. WILSON – PT. LOMA
(CALIFORNIA)
Transmitting Antenna Height : 1710 meters
Pacific Ocean
Receiving Antenna : 30.5 meters
ELEVATION IN METERS
1,750
1,500
1,250
1,000
750
500
250
0
0
10
20
30
40
50
60
70
80
90
100
110
120
130
140
150
160
170
180
190
TOTAL DISTANCE 184.66 KILOMETERS
MT. WILSON
PT. LOMA

Figure 2

PROFILES OF PACIFIC COAST LINE-OF-SIGHT
PROPAGATION PATHS

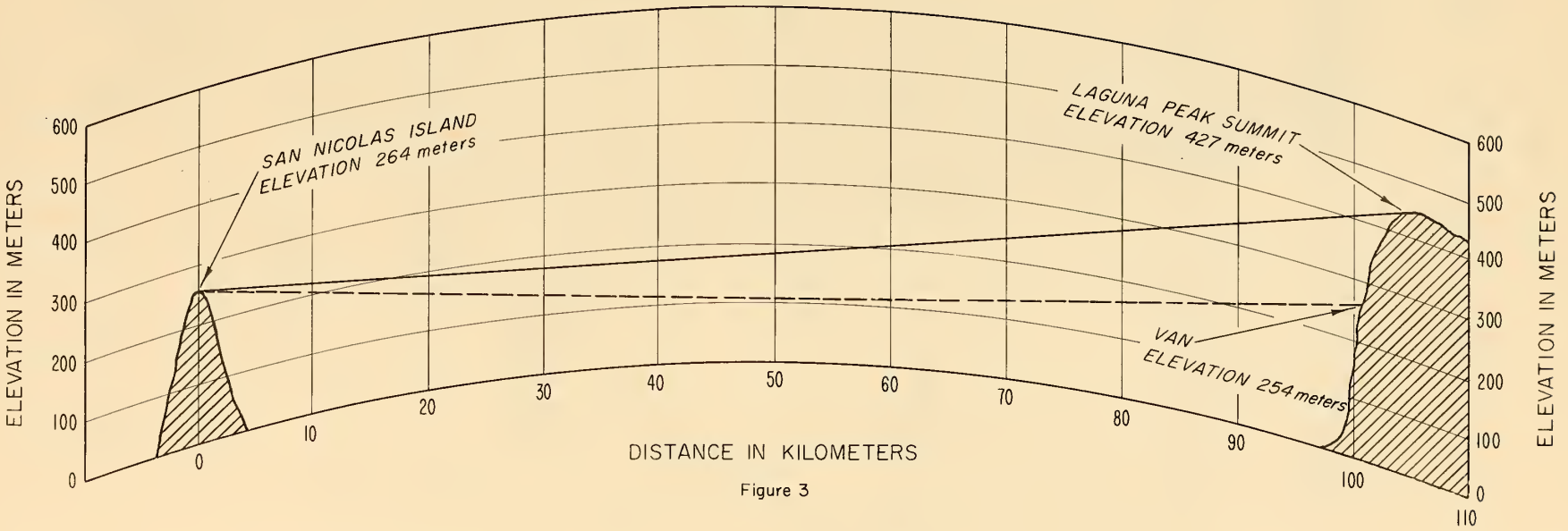


Figure 3

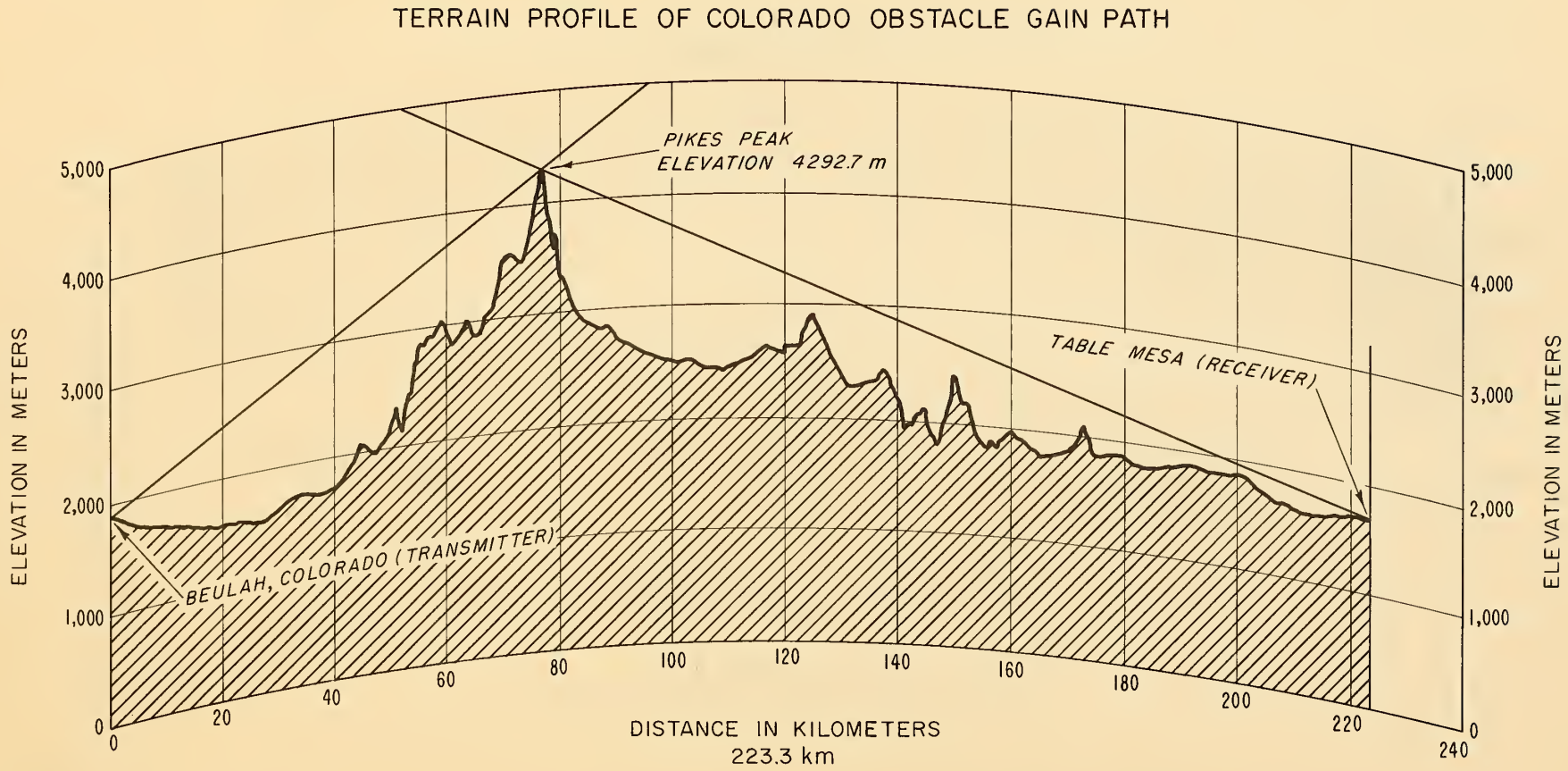
TERRAIN PROFILE OF COLORADO OBSTACLE GAIN PATH
PIKES PEAK
ELEVATION 4292.7 m
TABLE MESA (RECEIVER)
BEULAH, COLORADO (TRANSMITTER)
ELEVATION IN METERS
5,000
4,000
3,000
2,000
1,000
0
0
20
40
60
80
100
120
140
160
180
200
220
240
DISTANCE IN KILOMETERS
223.3 km

Figure 4

# TYPICAL PROLONGED SPACE-WAVE FADEOUT

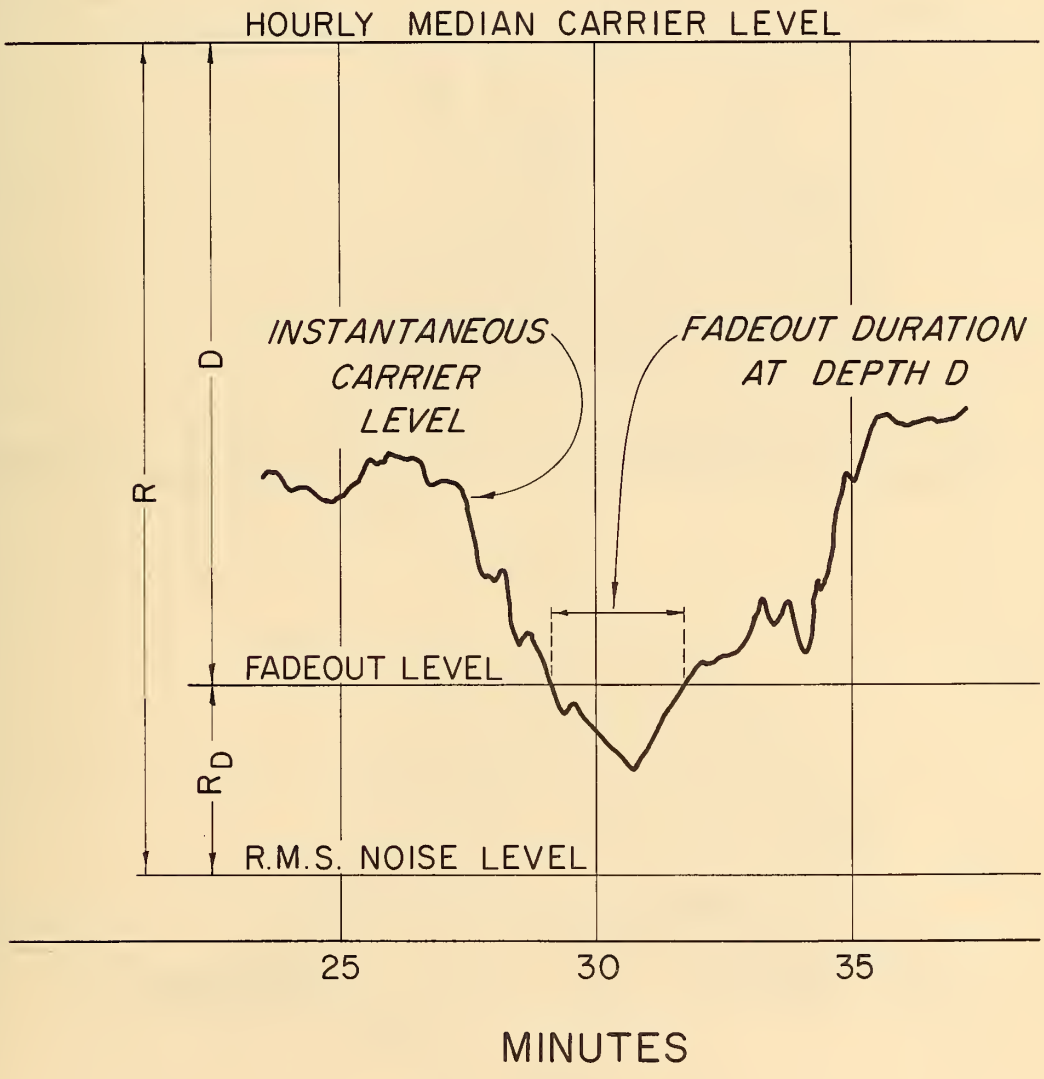


Figure 5

RECORDING CHART SAMPLE FOR CHEYENNE MOUNTAIN—KARVAL
WITHIN-THE-HORIZON PATH
1046 Mc

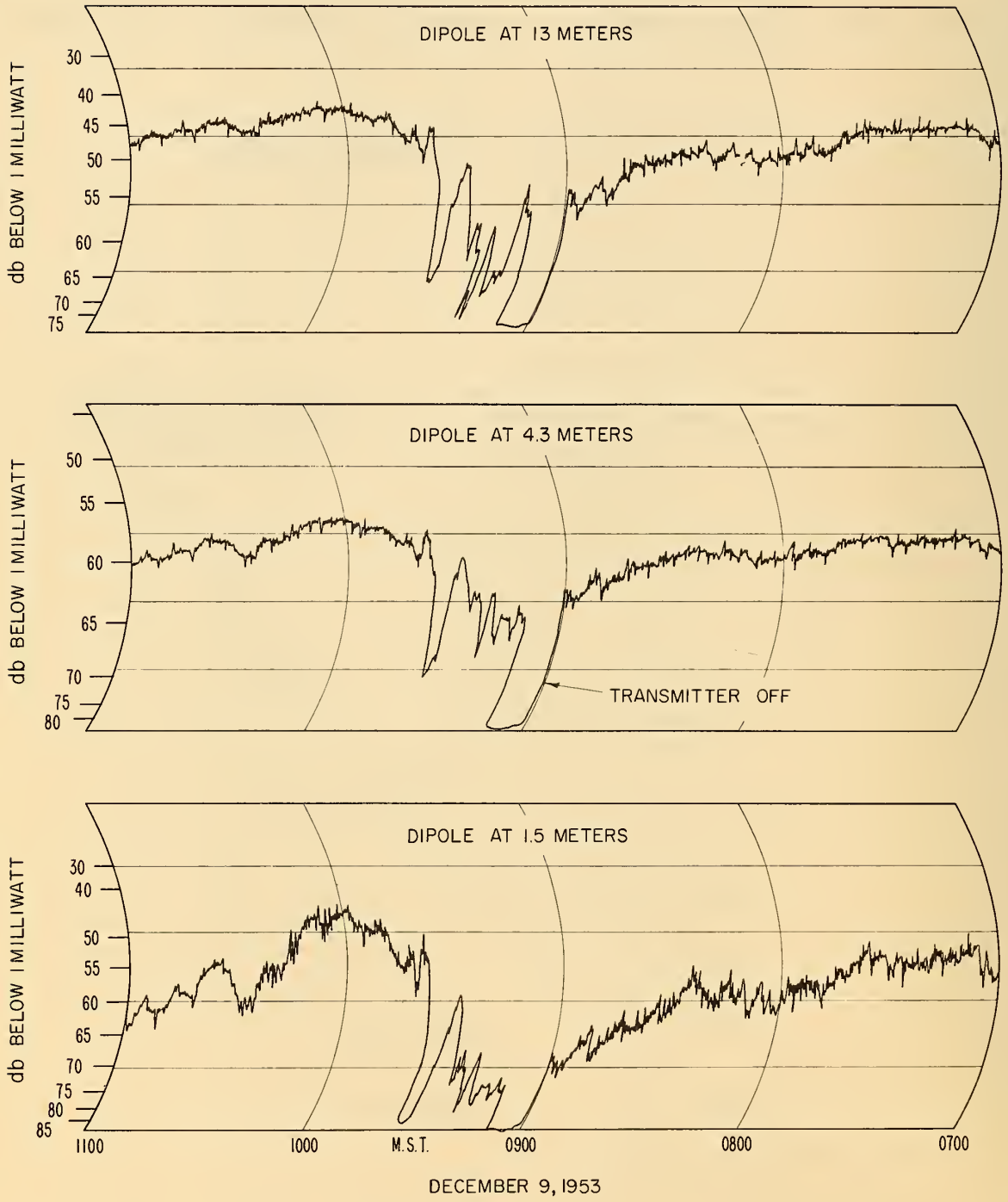


Figure 6

COMPARISON OF THE DIURNAL DISTRIBUTIONS
OF PROLONGED SPACE-WAVE FADEOUTS
THAT OCCURRED AT 1046 MC AT KARVAL, COLORADO
FOR 1952 AND 1953

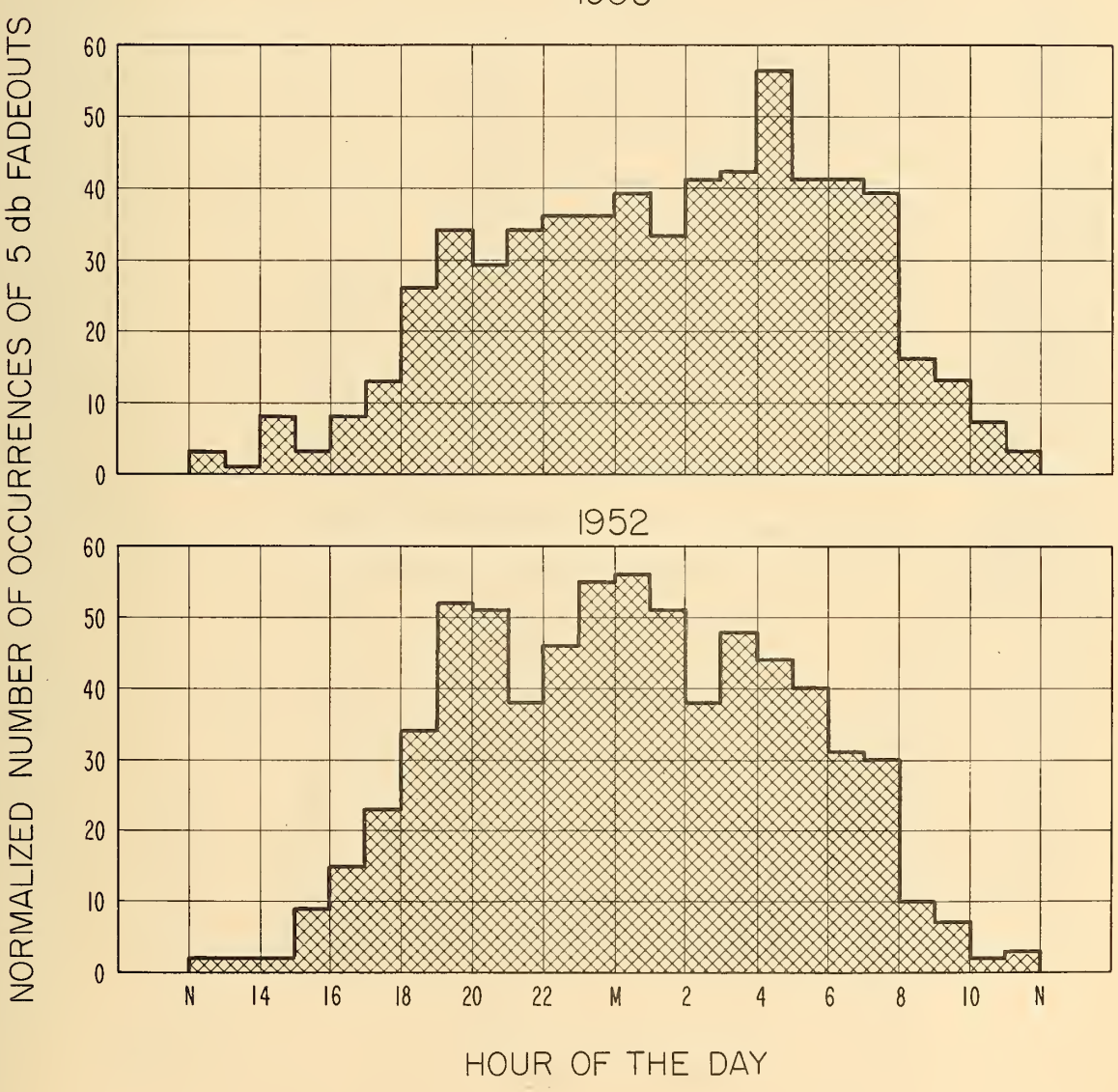


Figure 7

COMPARISON OF REFRACTIVITY PROFILES
OBTAINED ON THE N.B.S. 150 METER TOWER AT HASWELL, COLORADO
WITH THE OCCURRENCE OF PROLONGED SPACE-WAVE FADEOUTS AT KARVAL, COLORADO
DURING DECEMBER 13, 1953

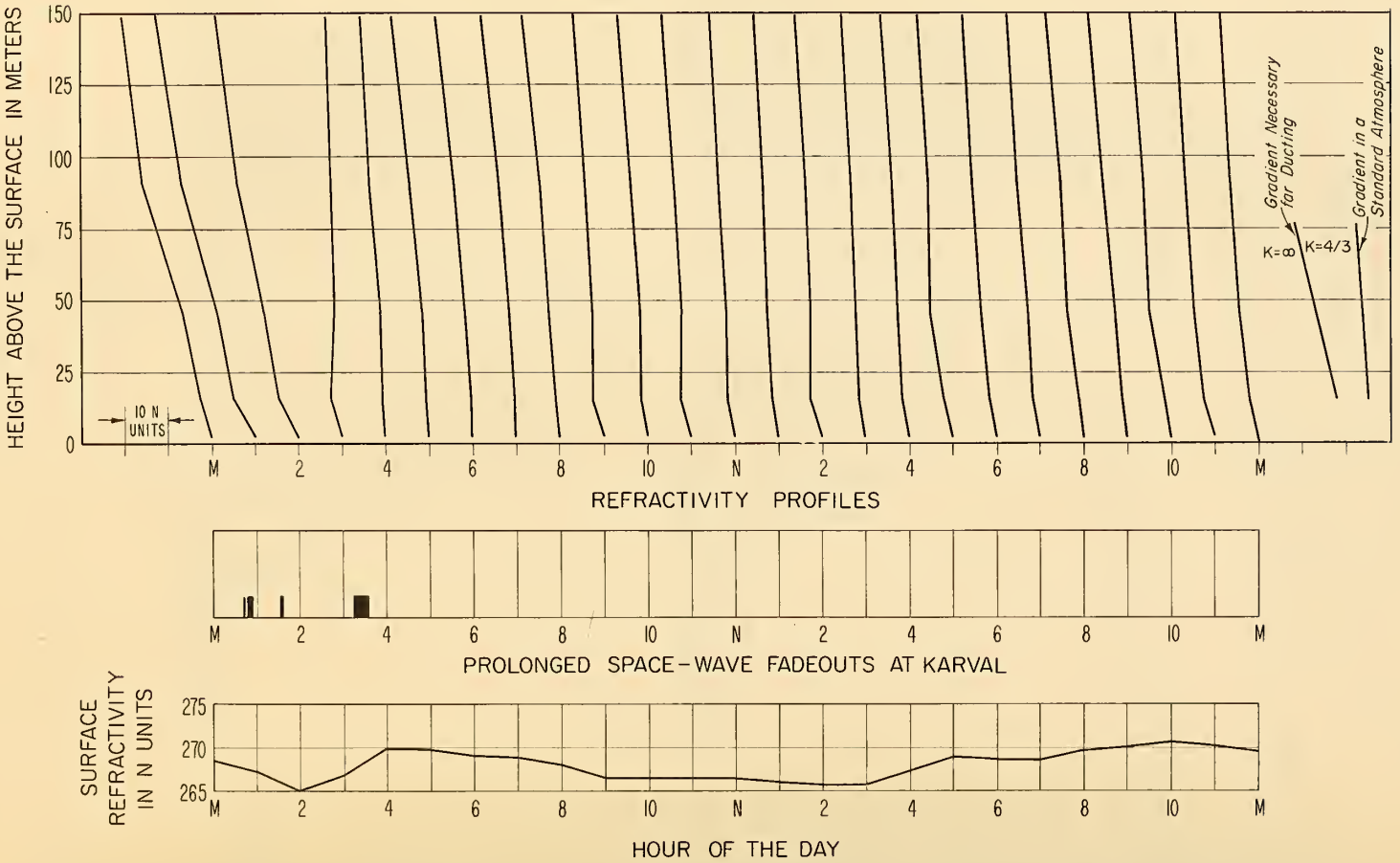


Figure 8

NORMALIZED NUMBER OF OCCURRENCES
OF 5db PROLONGED SPACE-WAVE FADEOUTS THAT OCCURRED
AT 1046 MC AT KARVAL, COLORADO DURING 1952-1953


Figure 9

PERCENTAGE OF TOTAL TIME FOR EACH MONTH THAT THE 1046 MC FIELD AT KARVAL, COLORADO IS AT LEAST 5 db AND 10 db BELOW THE MONTHLY MEDIAN DUE TO PROLONGED SPACE-WAVE FADEOUTS DURING 1952 AND 1953

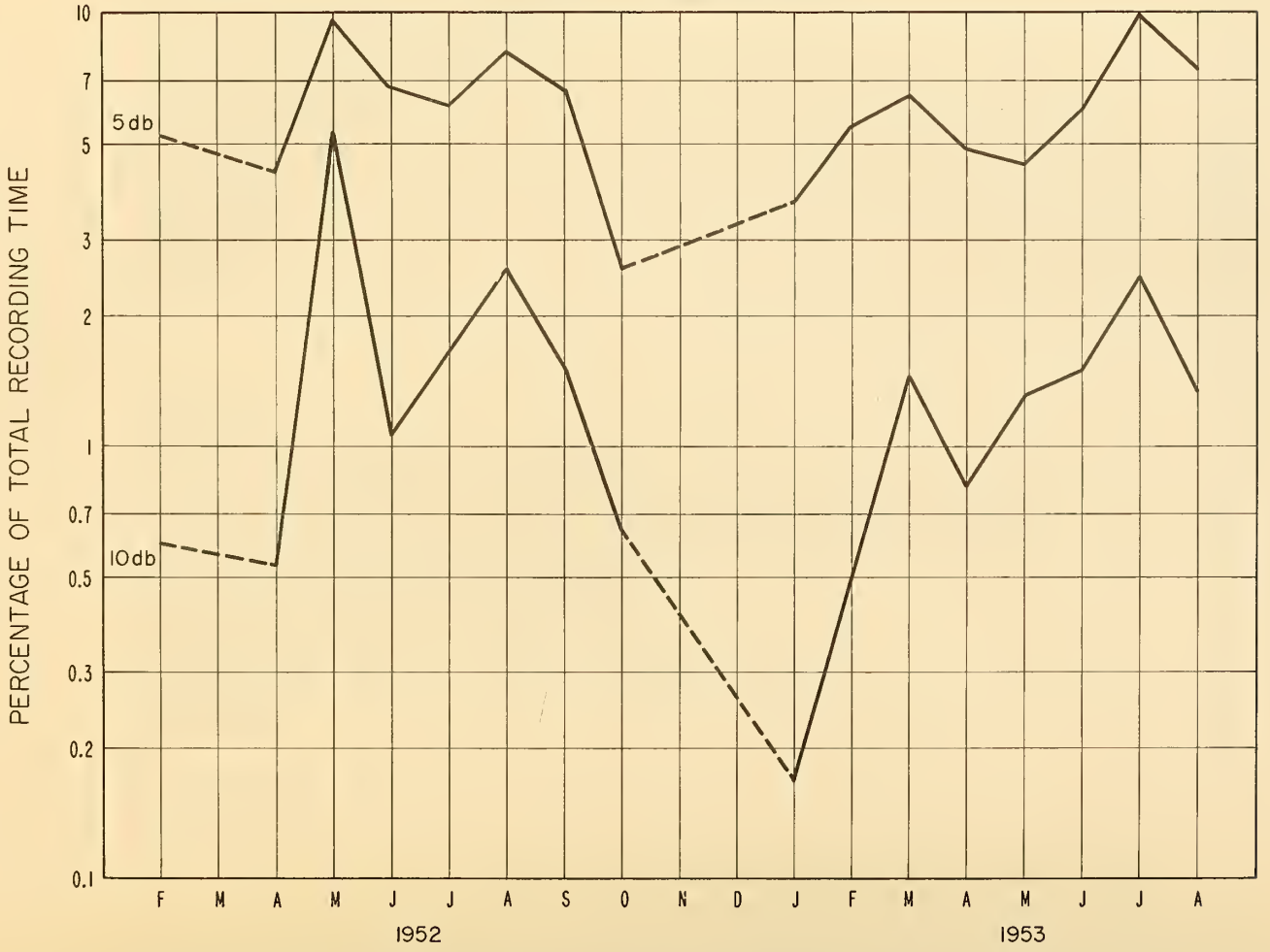


Figure 10

CUMULATIVE DISTRIBUTIONS OF THE PROLONGED SPACE-WAVE FADEOUTS THAT ARE AT LEAST 5, 10, AND 15 db BELOW THE MONTHLY MEDIAN FIELD AT 1046 MC AT KARVAL, COLORADO, 1952 AND 1953

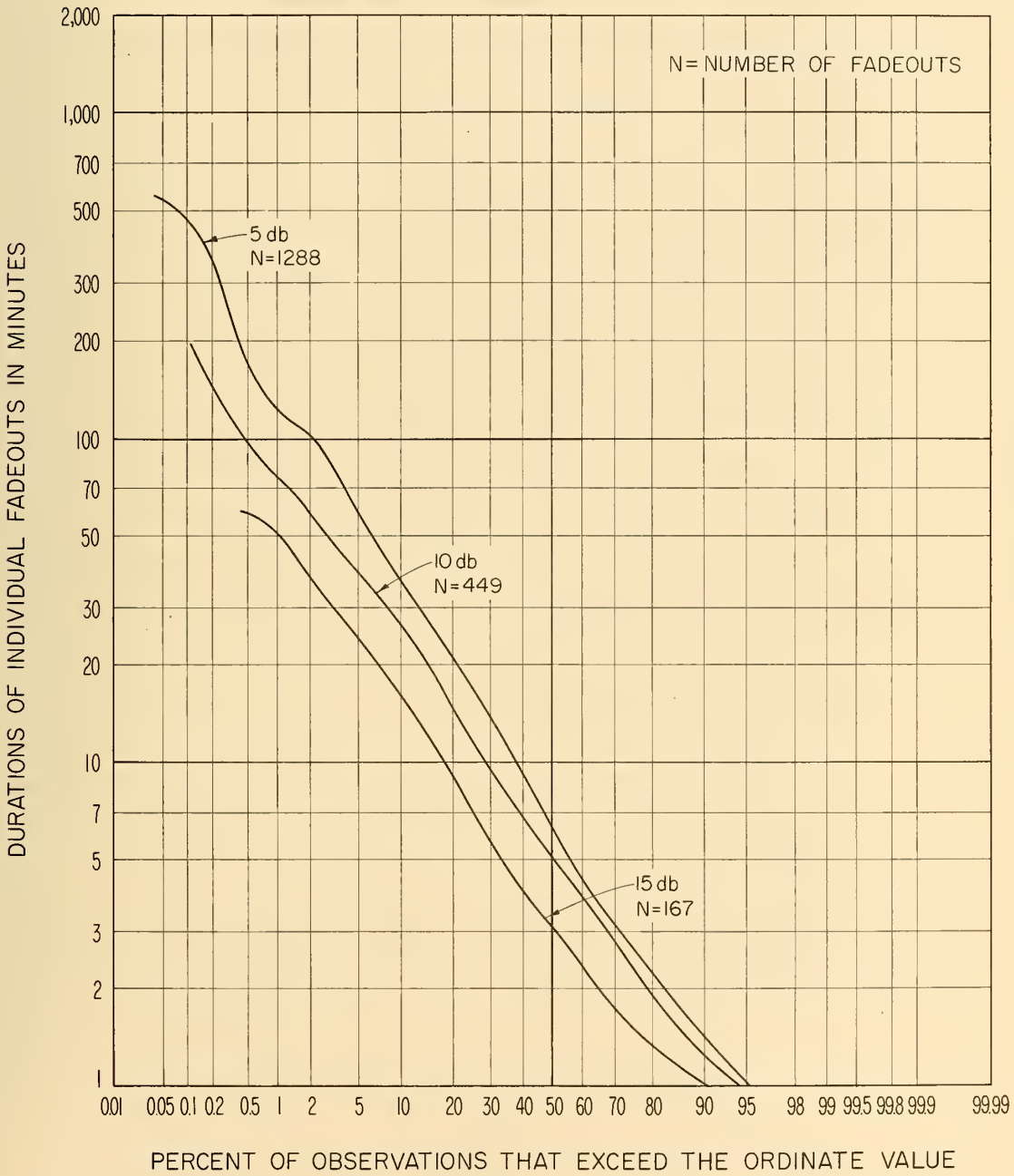


Figure 11

DISTRIBUTION OF FADEOUT DURATIONS FOR
VARIOUS LEVELS BELOW THE MONTHLY MEDIANS

1046 Mc, CHEYENNE MOUNTAIN - KARVAL PATH
FEBRUARY 1952 - AUGUST 1953

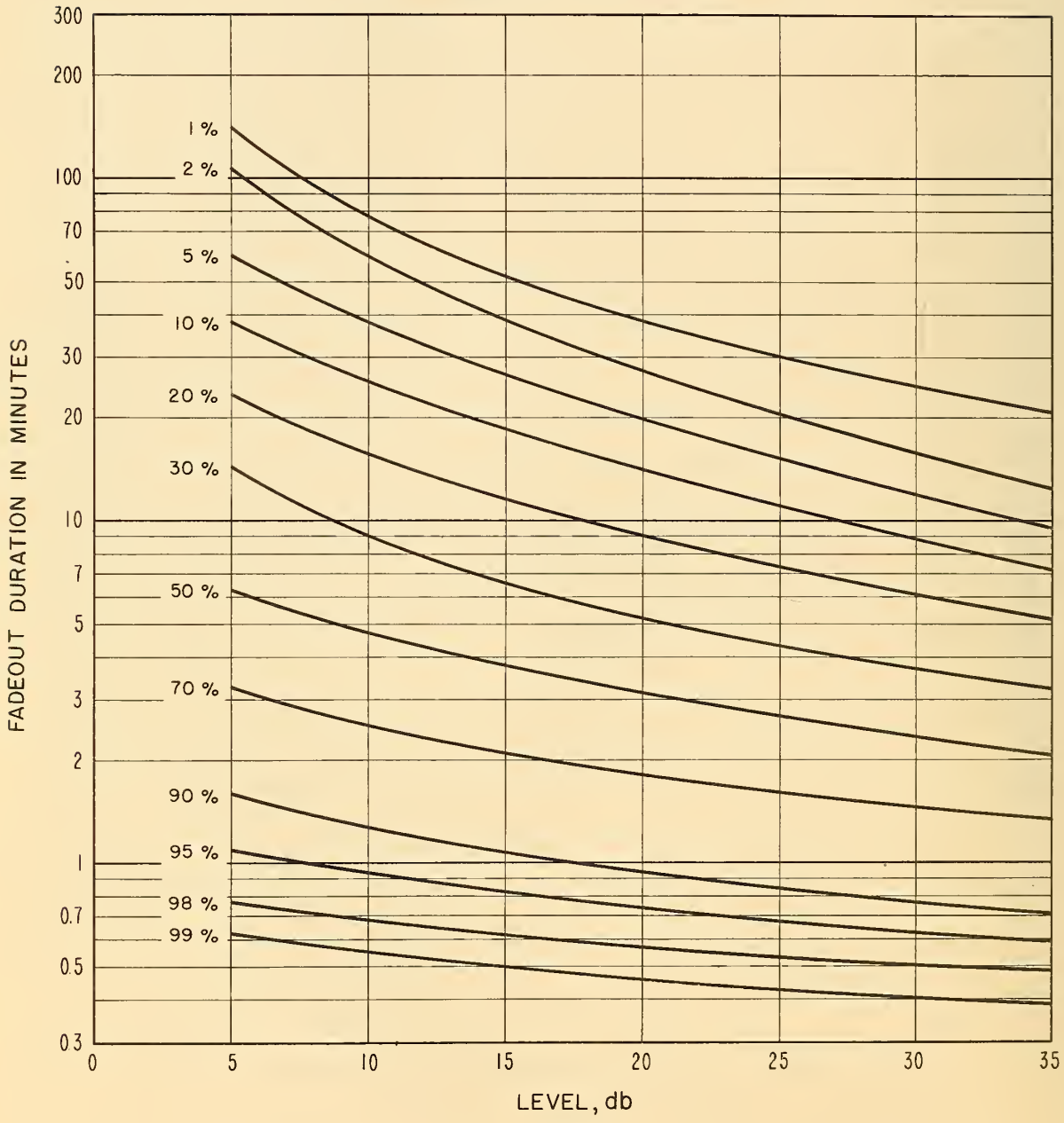


Figure 12

DISTRIBUTION OF PROLONGED SPACE WAVE FADEOUTS
CHEYENNE MOUNTAIN – KARVAL PATH
1046 Mc, DECEMBER, 1953

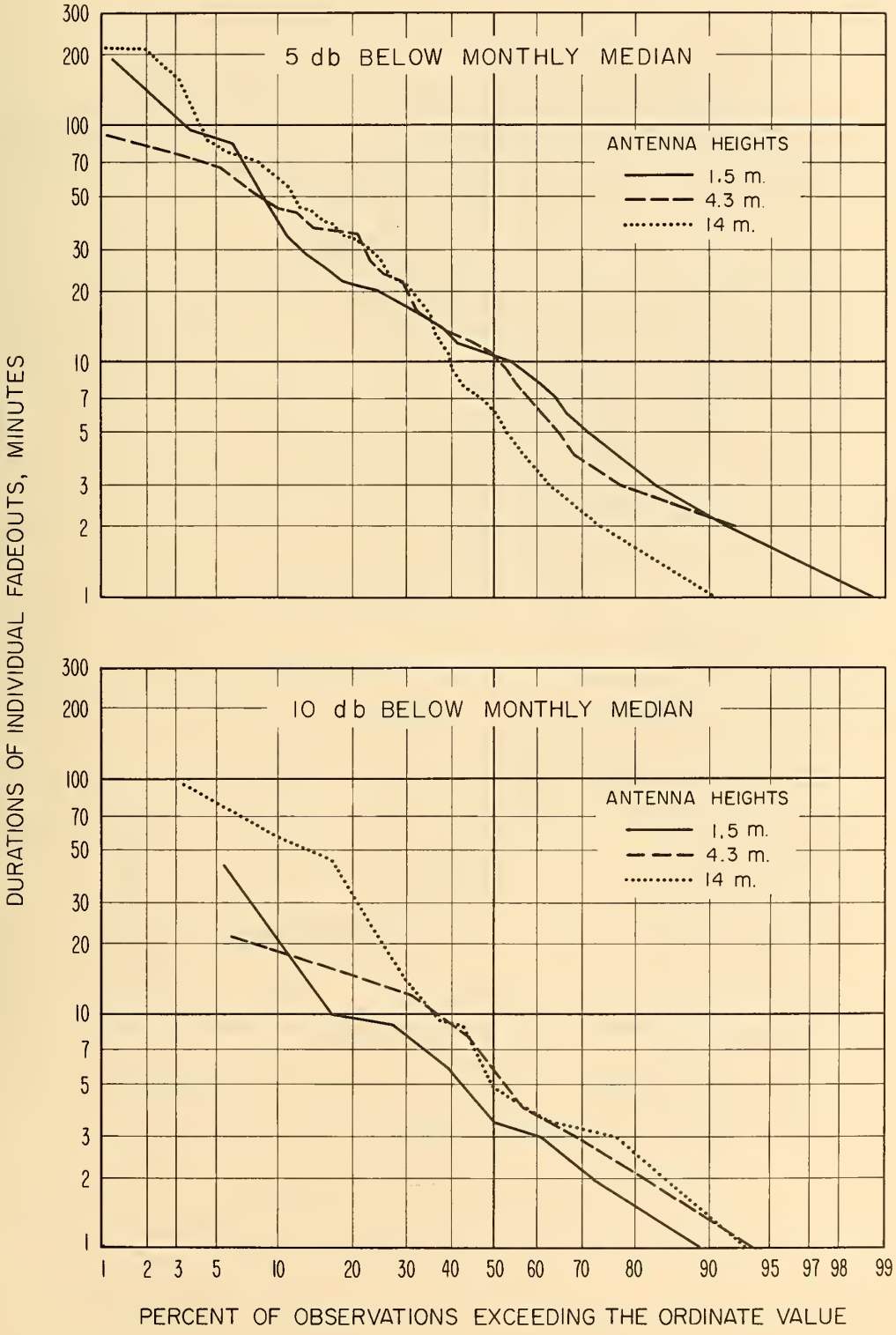


Figure 13

MAXIMUM DEPTH OF FADEOUTS IN DECIBELS
BELOW THE MONTHLY MEDIAN FIELD FOR KARVAL, COLORADO
AT ANTENNA HEIGHTS 1.5, 4.3 AND 14 METERS, DECEMBER, 1953

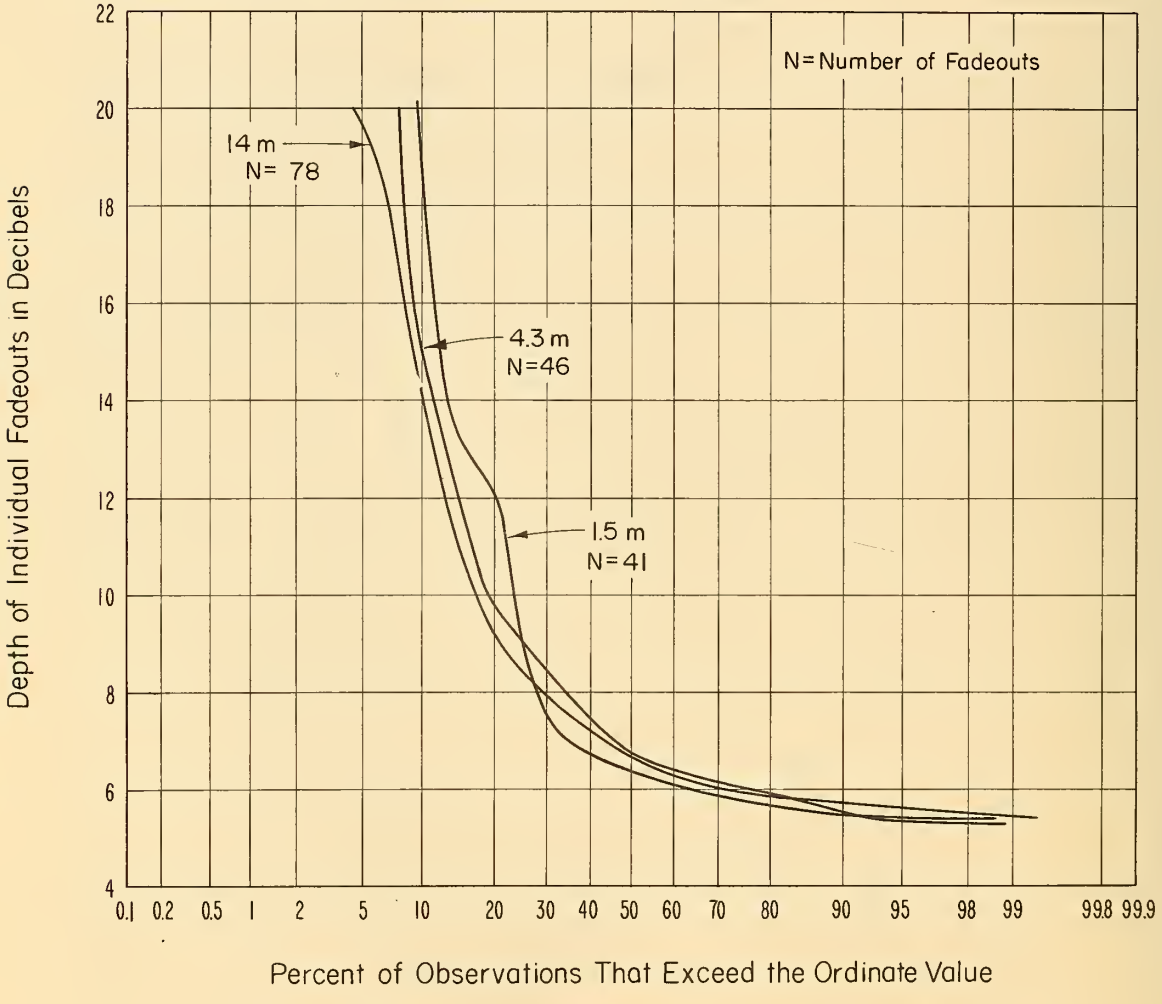


Figure 14

DIURNAL DISTRIBUTION OF THE NUMBER OF OCCURRENCES
OF 5db PROLONGED SPACE-WAVE FADEOUTS ON 138 MC AND 1250 MC
MT. WILSON TO N.E.L. (FIELD HOUSE)

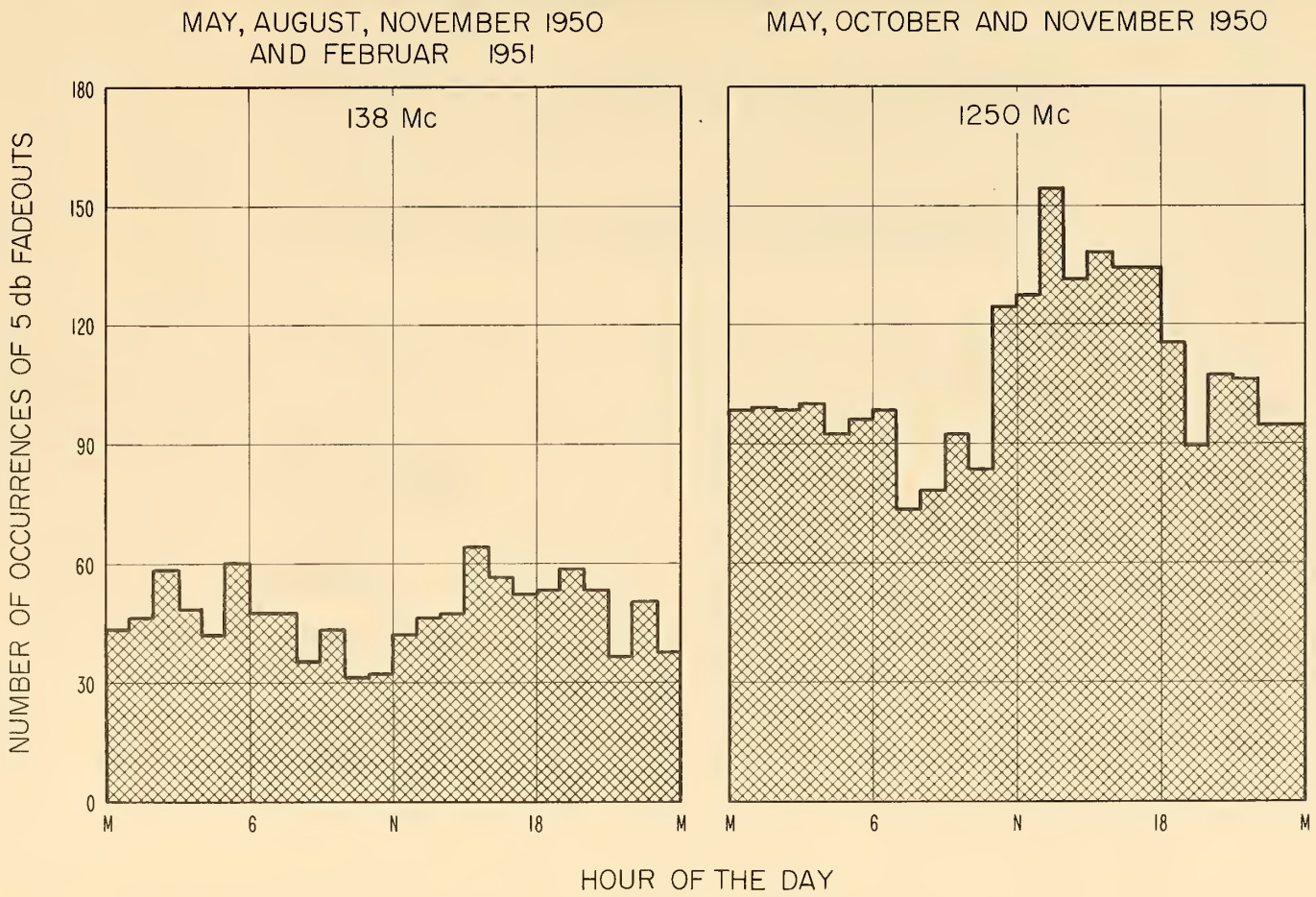


Figure 15

NORMALIZED NUMBER OF OCCURRENCES OF 5 db SPACE-WAVE FADEOUTS
MT. WILSON - PT. LOMA, 138 AND 1250 Mc PROPAGATION PATHS

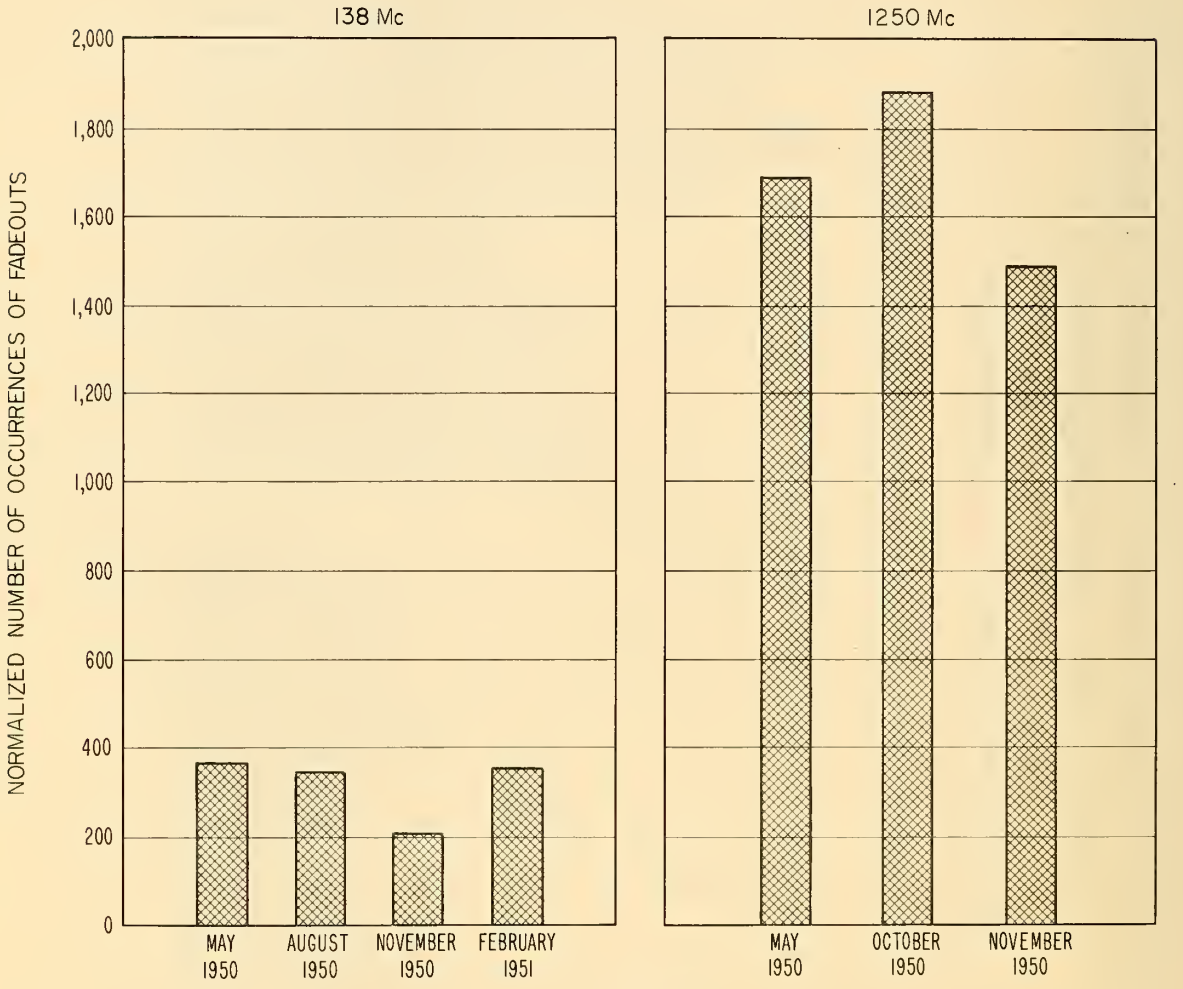


Figure 16

# CUMULATIVE DISTRIBUTIONS OF PROLONGED SPACE-WAVE FADEOUTS FOR THE MT. WILSON - POINT LOMA PROPAGATION PATH

MAY, AUGUST, NOVEMBER, 1950 AND FEBRUARY, 1951
FADEOUT LEVELS RELATIVE TO MONTHLY MEDIAN

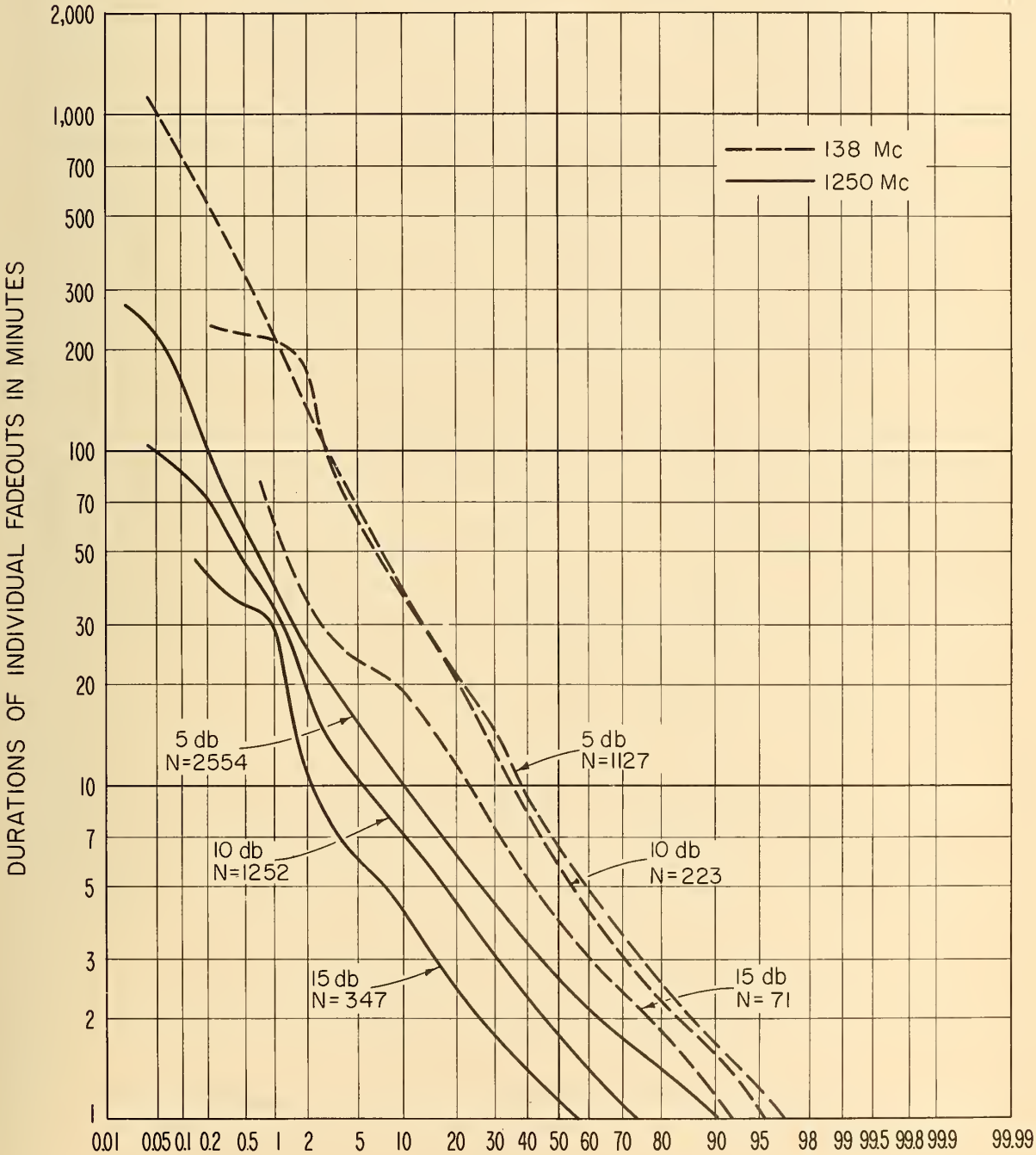


Figure 17

DISTRIBUTIONS OF FADEOUT DURATIONS FOR LEVELS BELOW THE MONTHLY MEDIANS

MOUNT WILSON — POINT LOMA PATH
1950 – 1951

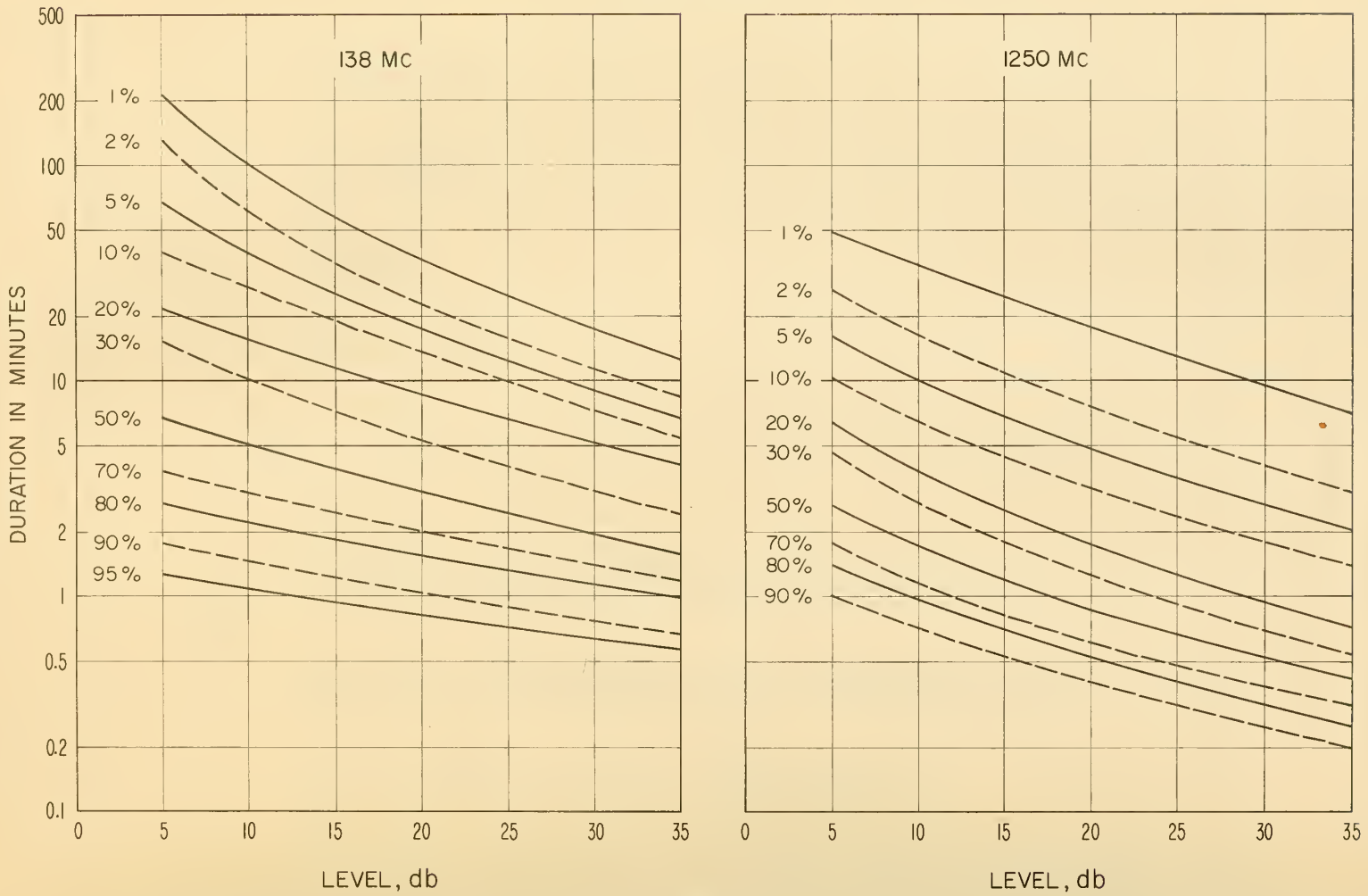


Figure 18

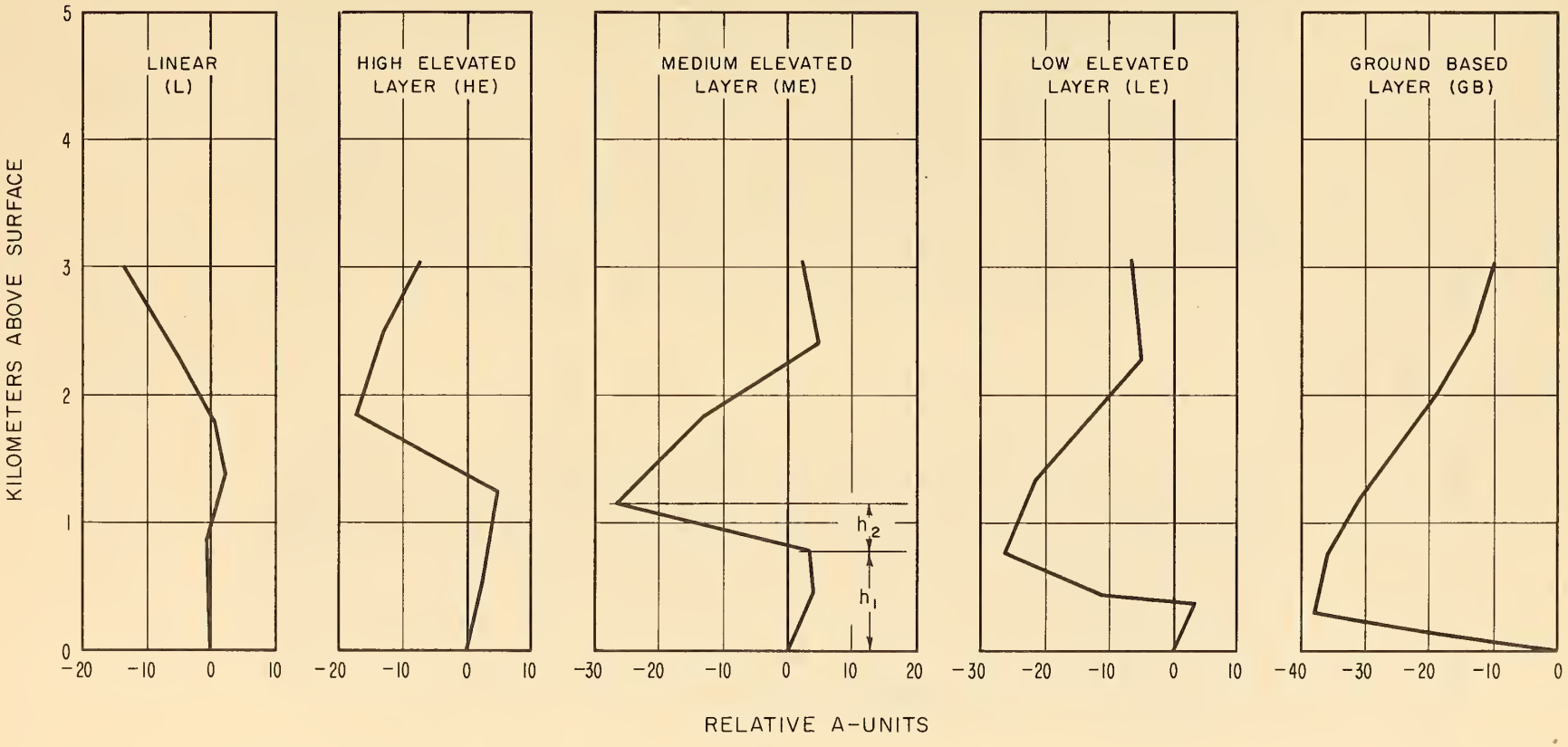
CHARACTERISTIC TYPES OF REFRACTIVE INDEX PROFILES
KILOMETERS ABOVE SURFACE
LINEAR (L)
HIGH ELEVATED LAYER (HE)
MEDIUM ELEVATED LAYER (ME)
LOW ELEVATED LAYER (LE)
GROUND BASED LAYER (GB)
h2
h1
RELATIVE A-UNITS

Figure 19

SAMPLES OF 394 MC RECORD FOR WITHIN-THE-HORIZON PATH
SAN NICOLAS ISLAND-LAGUNA PEAK

(a) Linear Refractive Index Profile, No Space-Wave Fadeouts

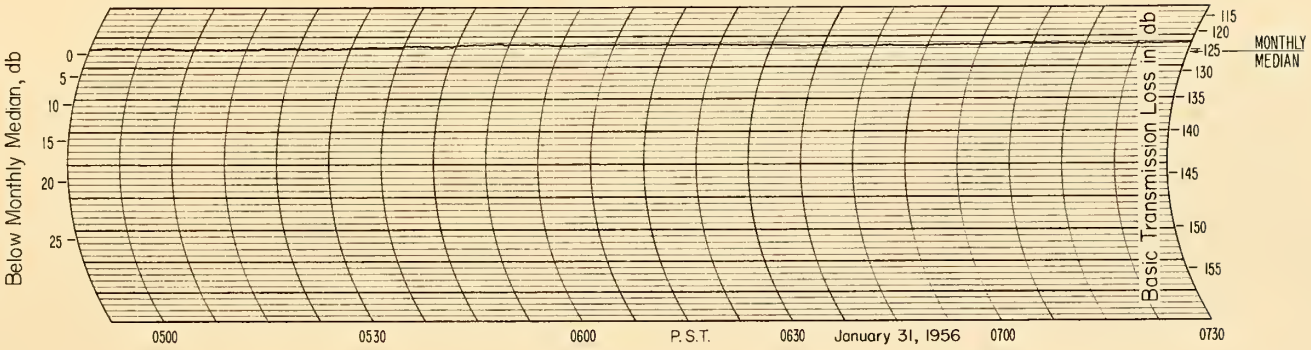


(b) Refractive Index Profile Characterized by a Ground Based Layer, Pronounced Space-Wave Fadeouts

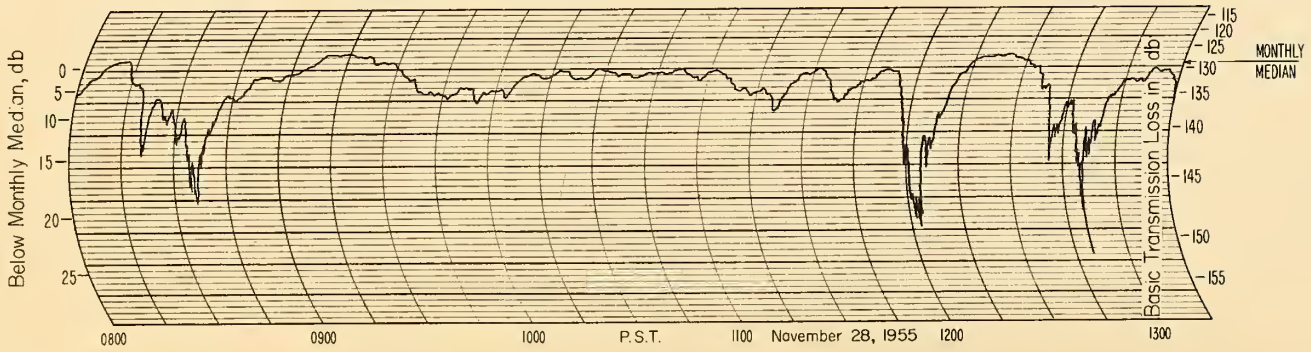


Figure 20

# PERCENT FADEOUT TIME AS A FUNCTION OF PROFILE CHARACTERISTICS SAN NICOLAS ISLAND—LAGUNA PEAK (SUMMIT) PERIOD NOVEMBER 1955—OCTOBER 1957

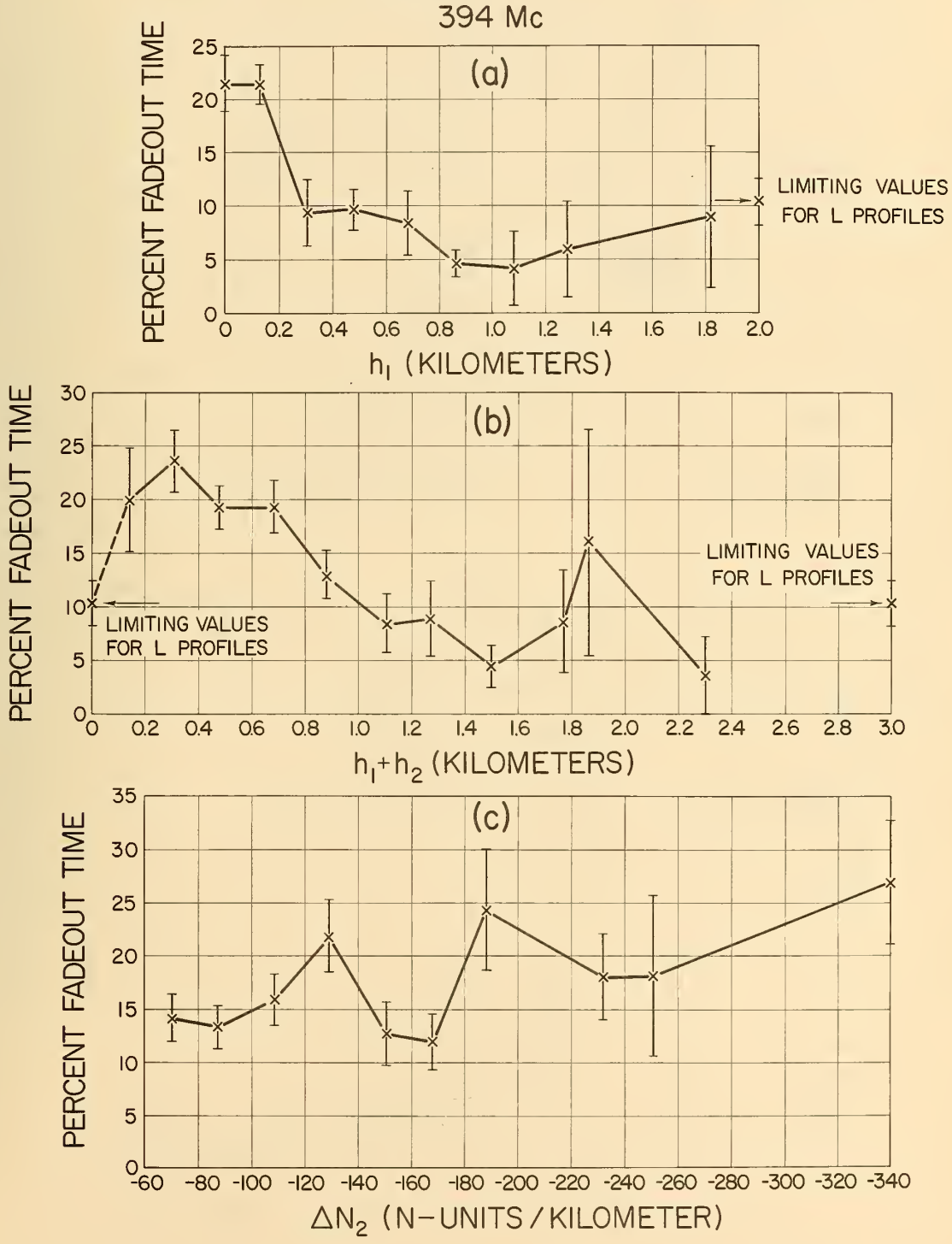


Figure 21

# FADEOUT OCCURENCE AS A FUNCTION OF FREQUENCY
## SAN NICOLAS ISLAND – LAGUNA PEAK

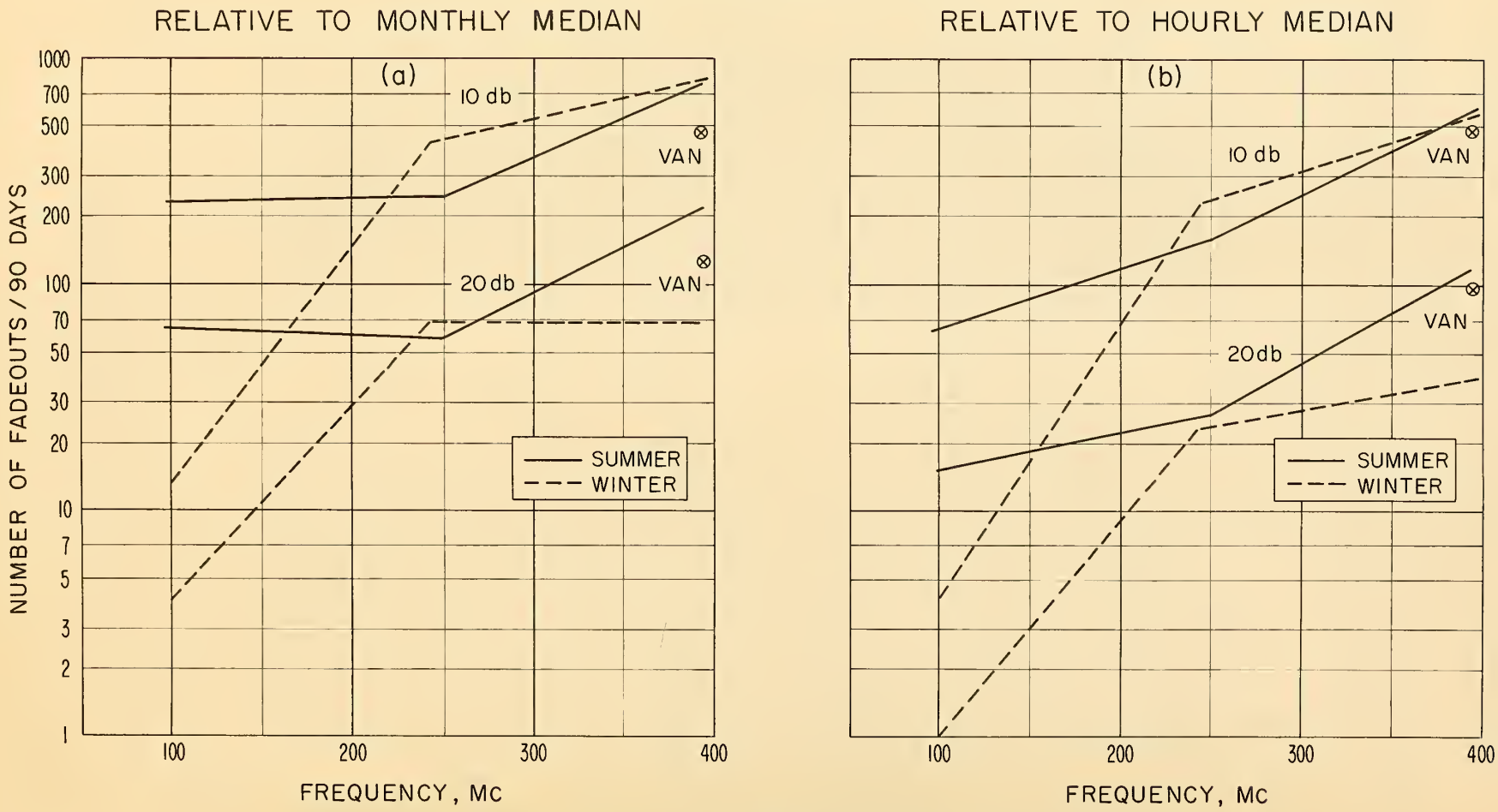


Figure 22

FADEOUT INCIDENCE FOR SAN NICOLAS ISLAND - LAGUNA PEAK PATH

APRIL - AUGUST, 1959

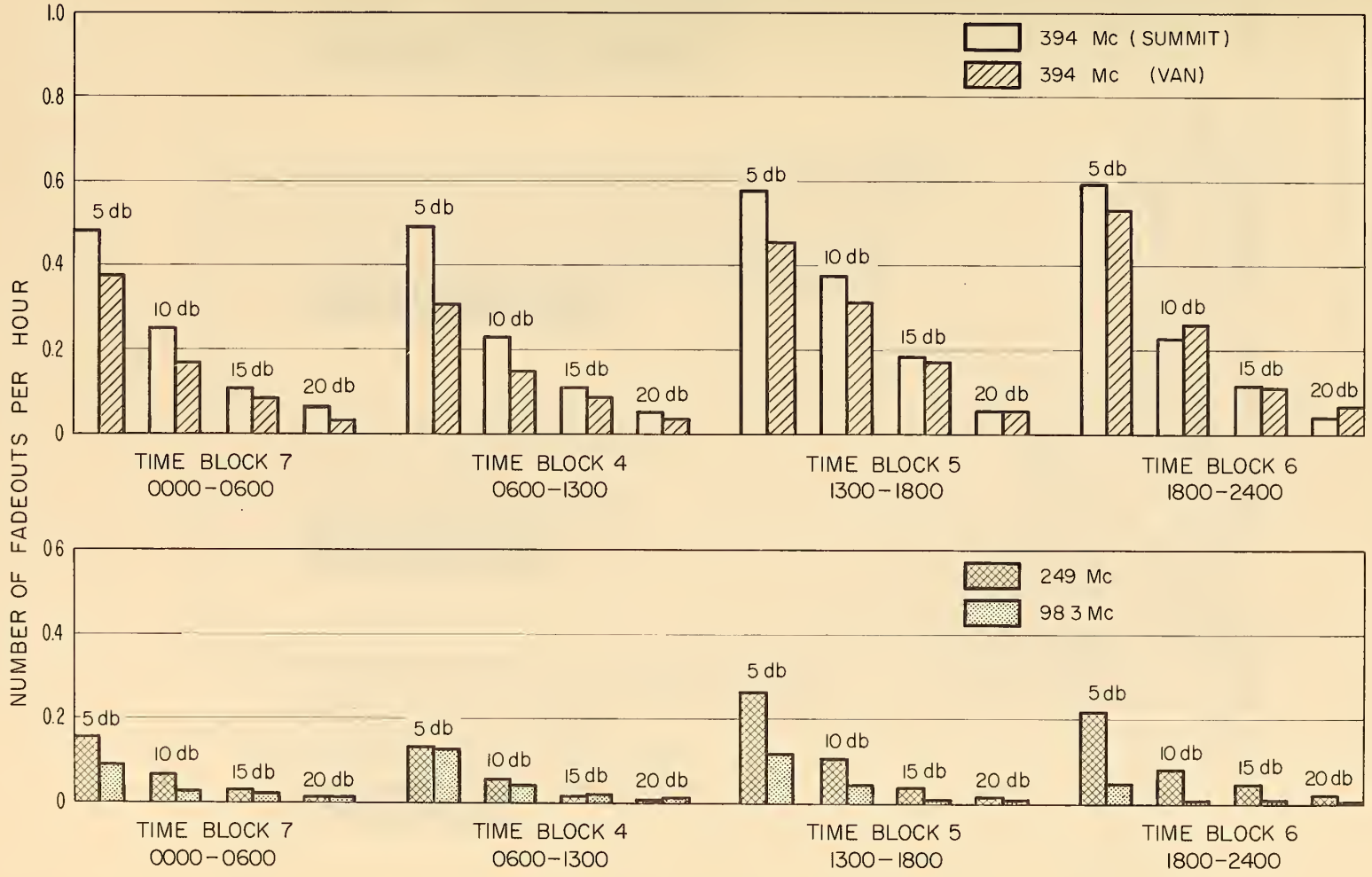


Figure 23

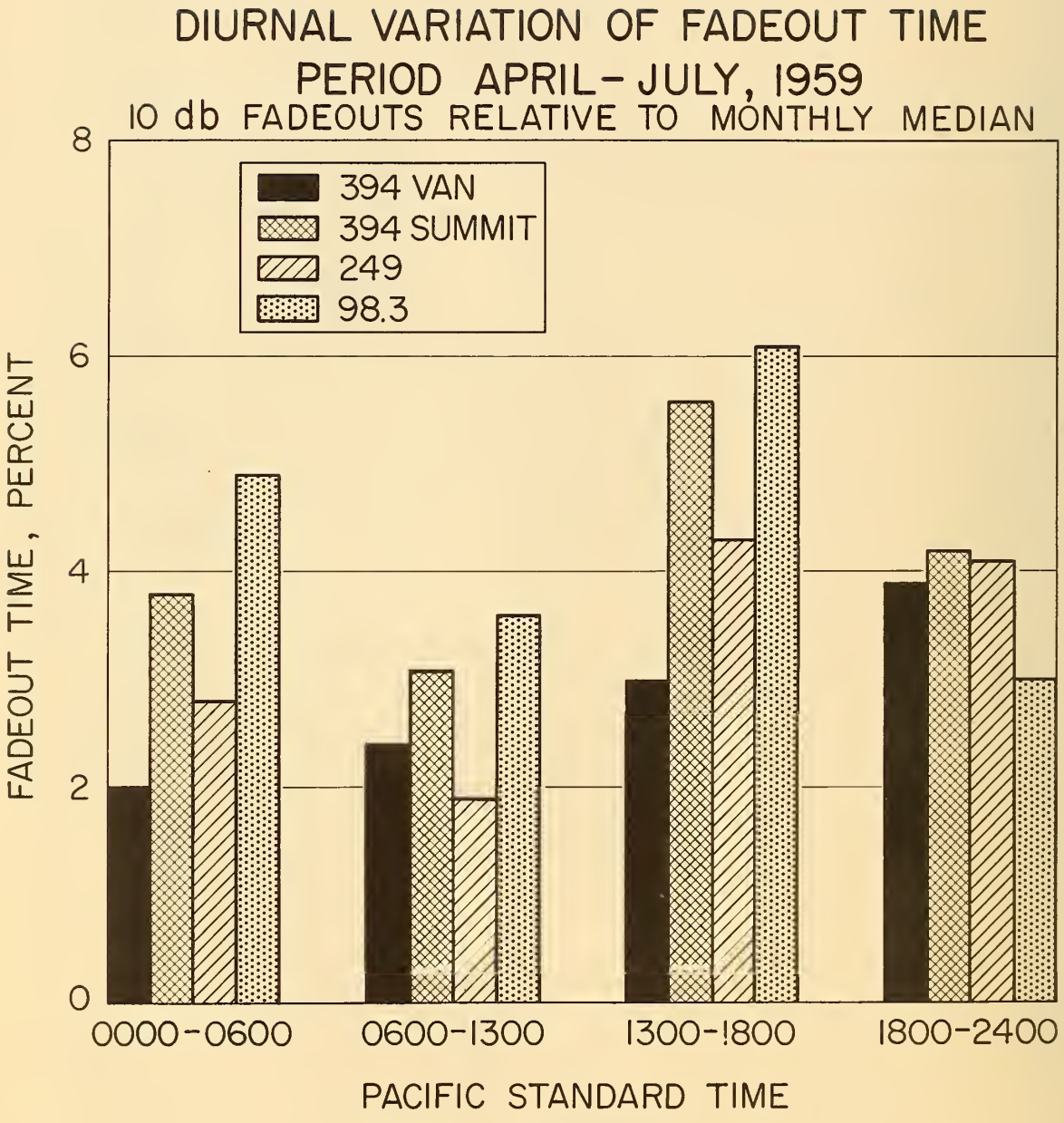
DIURNAL VARIATION OF FADEOUT TIME
PERIOD APRIL-JULY, 1959
10 db FADEOUTS RELATIVE TO MONTHLY MEDIAN
394 VAN
394 SUMMIT
249
98.3
FADEOUT TIME, PERCENT
0
2
4
6
8
0000-0600
0600-1300
1300-1800
1800-2400
PACIFIC STANDARD TIME

Figure 24

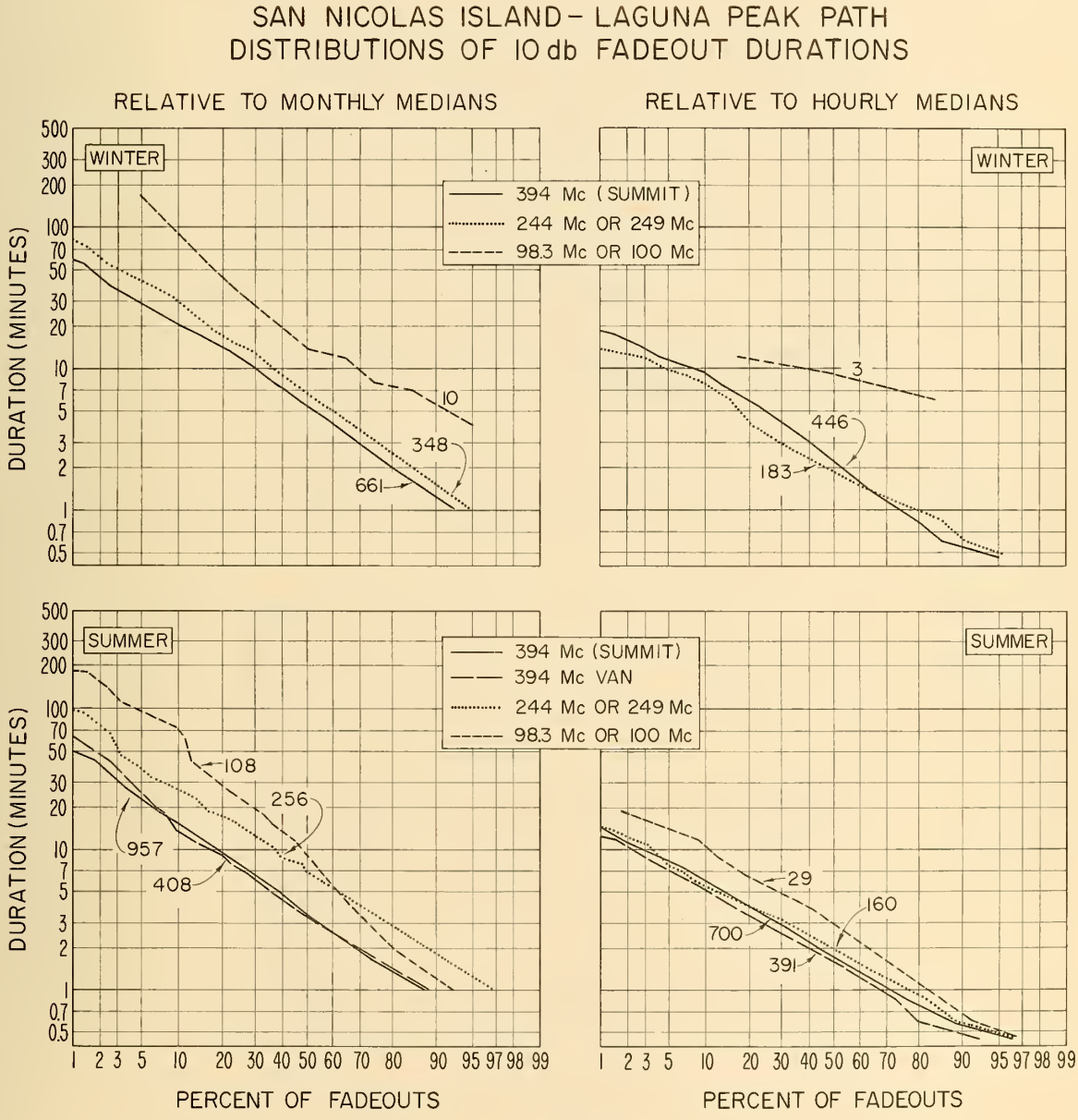
SAN NICOLAS ISLAND – LAGUNA PEAK PATH
DISTRIBUTIONS OF 10 db FADEOUT DURATIONS
RELATIVE TO MONTHLY MEDIANS
RELATIVE TO HOURLY MEDIANS
WINTER
SUMMER
394 Mc (SUMMIT)
394 Mc VAN
244 Mc OR 249 Mc
98.3 Mc OR 100 Mc
DURATION (MINUTES)
PERCENT OF FADEOUTS
500
300
200
100
70
50
30
20
10
7
5
3
2
1
0.7
0.5
1 2 3 5 10 20 30 40 50 60 70 80 90 95 97 98 99
10
348
661
3
446
183
108
256
957
408
29
160
700
391

Figure 25

DISTRIBUTION OF FADEOUT DURATIONS FOR
VARIOUS LEVELS BELOW THE HOURLY MEDIANS

394 MC, SAN NICOLAS ISLAND-LAGUNA PEAK PATH
APRIL-JULY, 1959

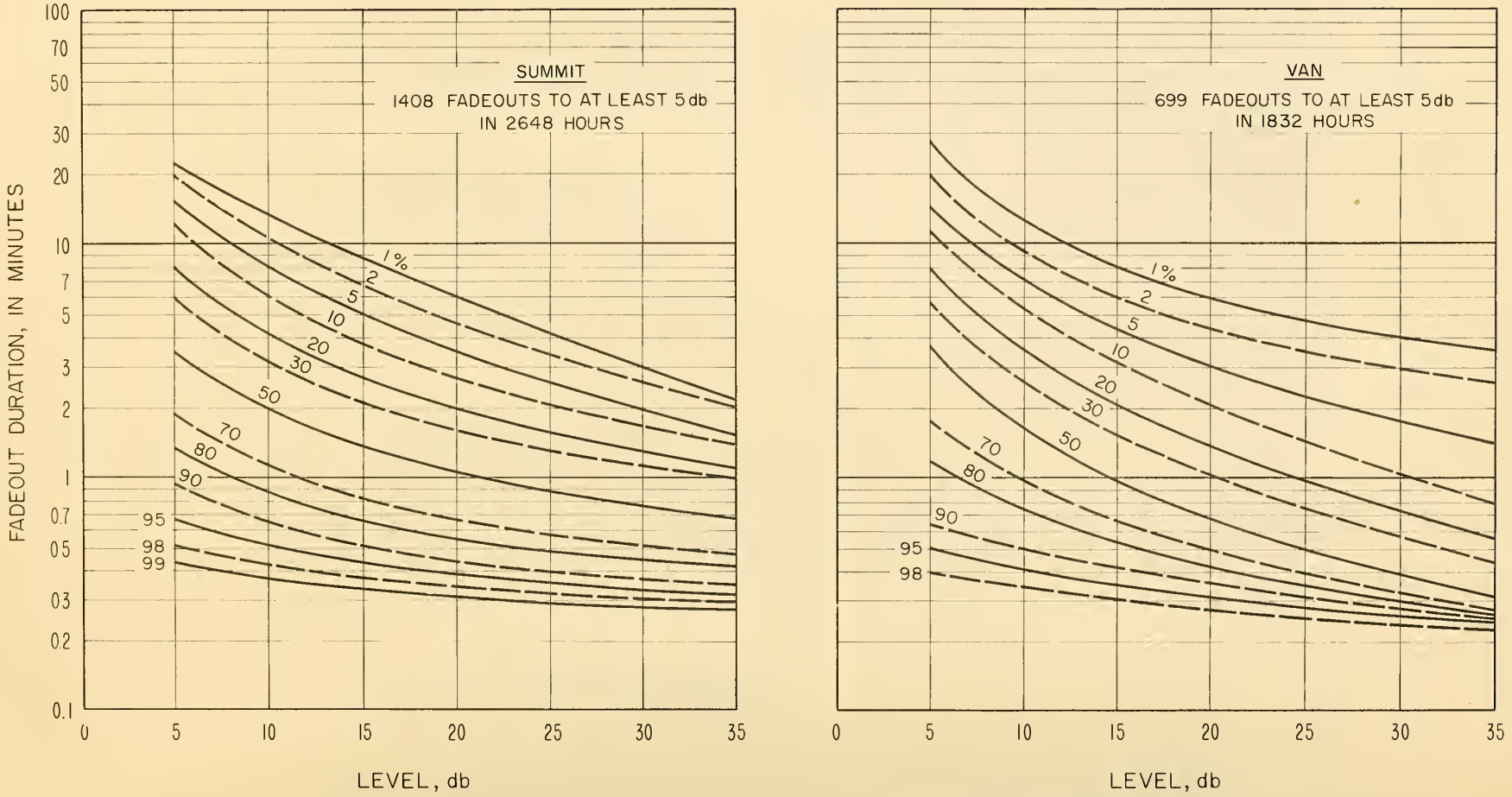


Figure 26

RECORDING CHART SAMPLES FOR COLORADO
OBSTACLE GAIN PATH
751 Mc

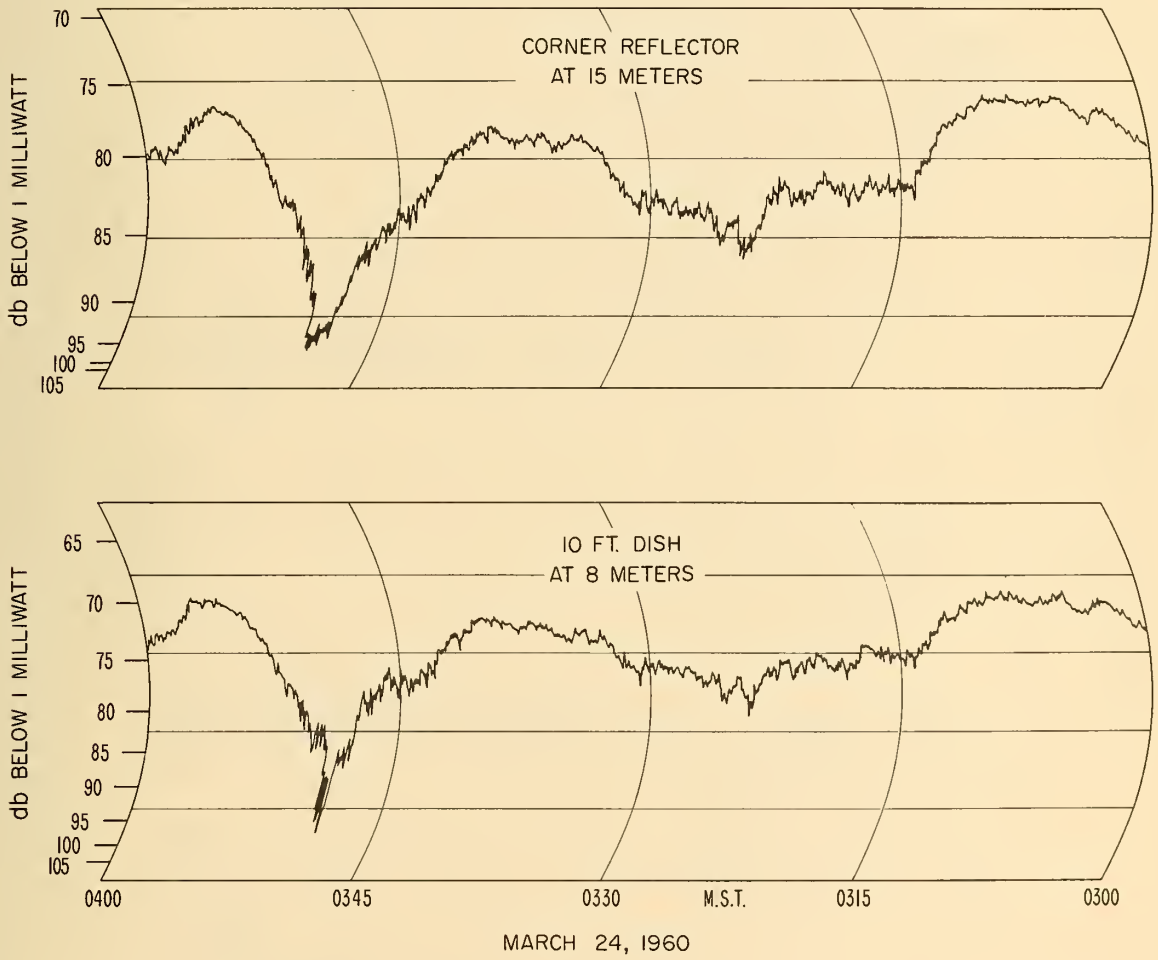


Figure 27

FADEOUT INCIDENCE FOR COLORADO
OBSTACLE GAIN PATH
751 Mc, JUNE – SEPTEMBER 1960

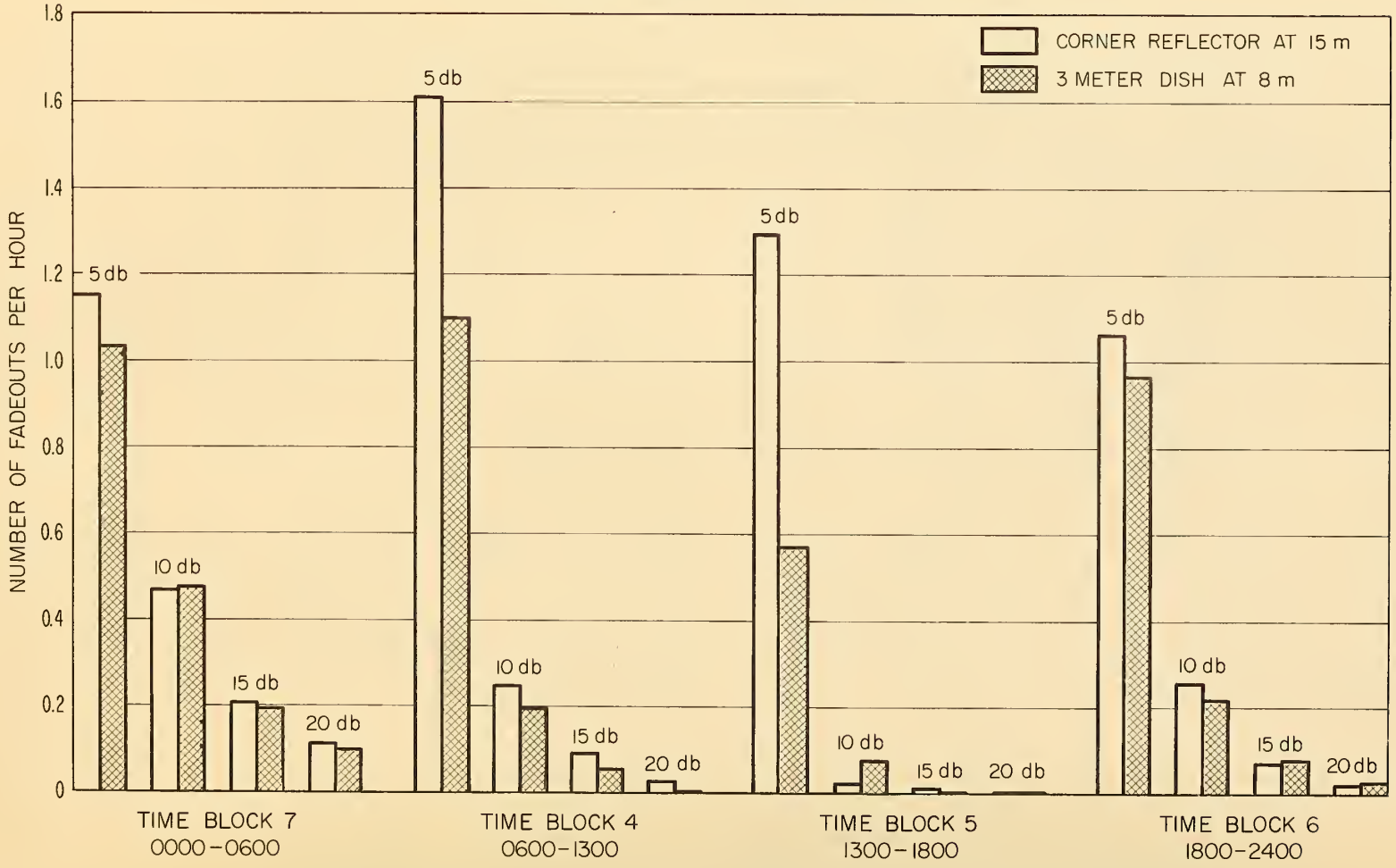


Figure 28

COLORADO OBSTACLE GAIN PATH

DISTRIBUTIONS OF FADEOUT DURATIONS AT VARIOUS LEVELS
BELOW THE HOURLY MEDIANS

751 Mc, SUMMER 1960

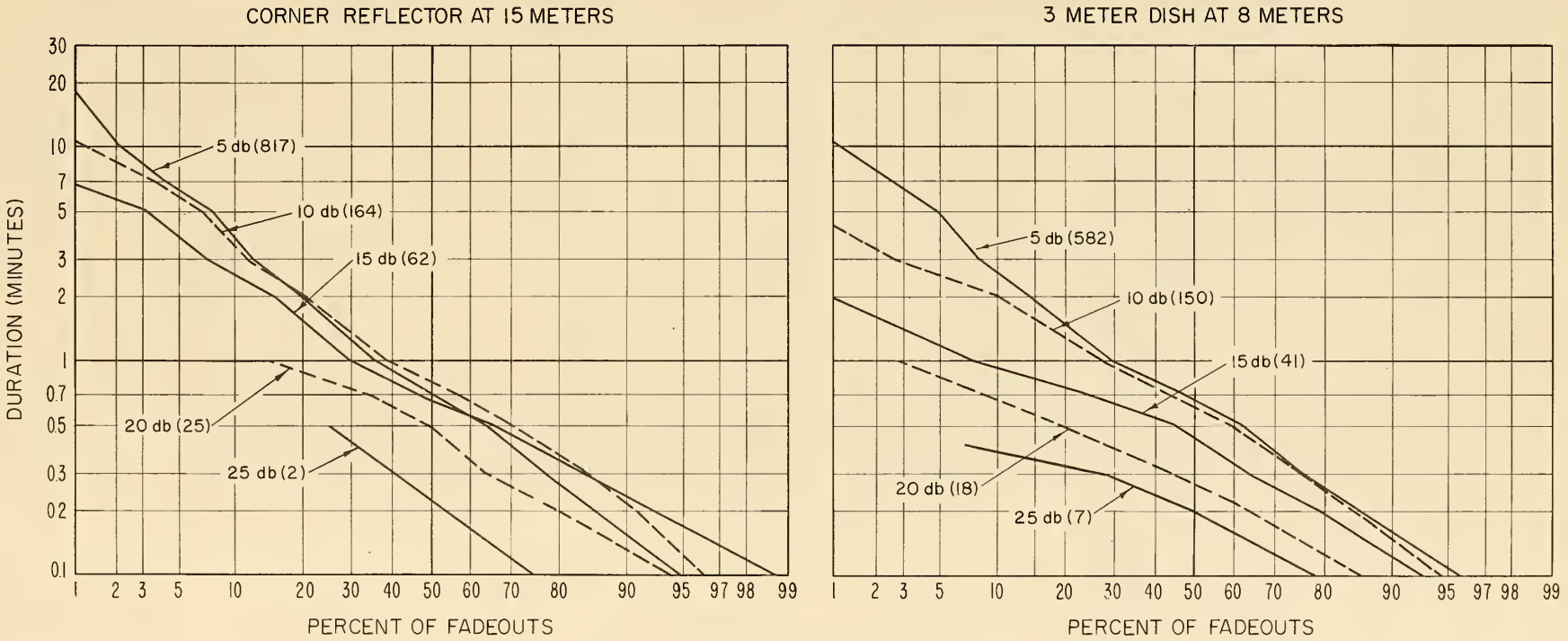


Figure 29

COLORADO OBSTACLE GAIN PATH

DISTRIBUTIONS OF FADEOUT DURATIONS AT VARIOUS LEVELS
BELOW THE HOURLY MEDIANS

751 MC, SUMMER 1960

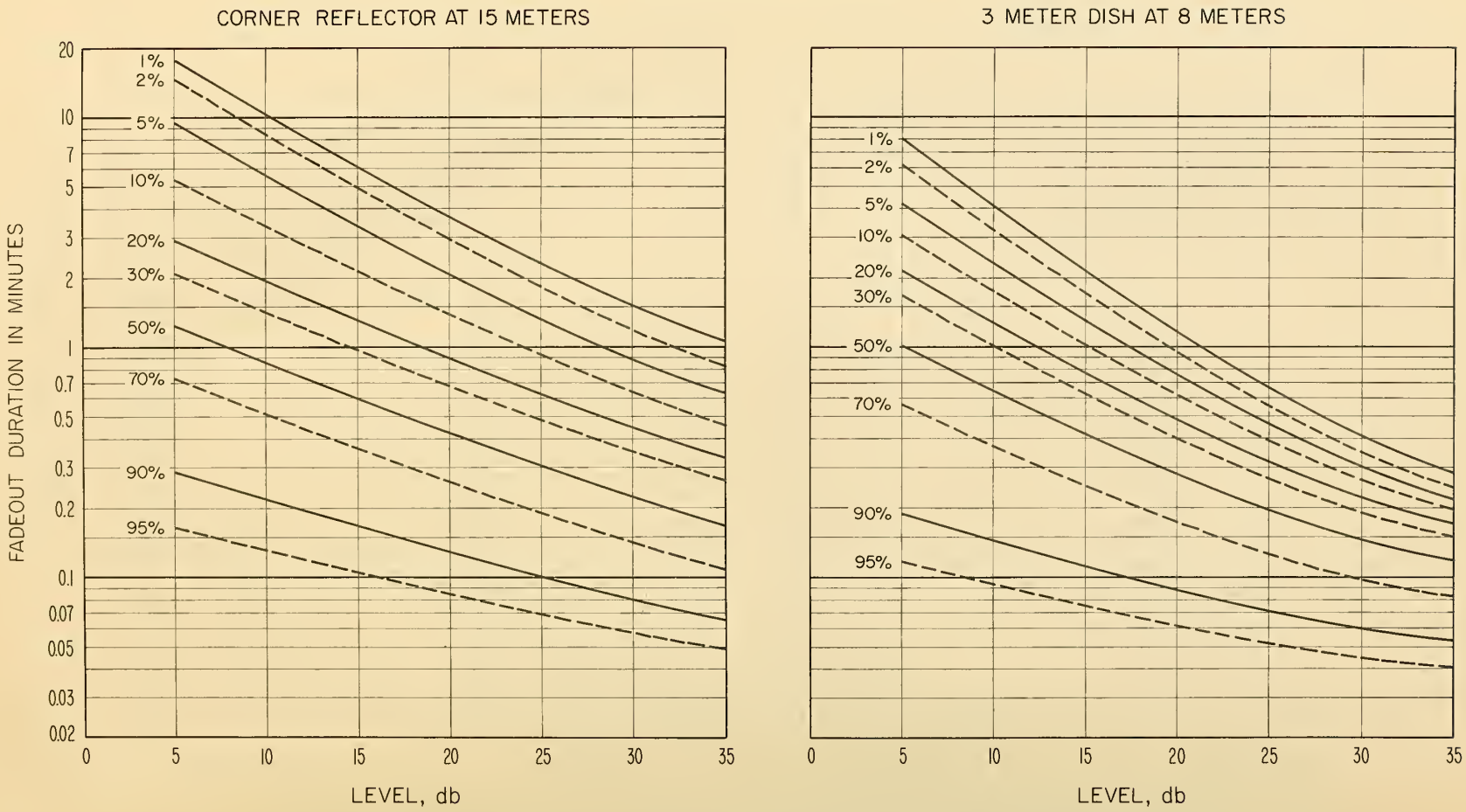


Figure 30

U.S. DEPARTMENT OF COMMERCE
Frederick H. Mueller, *Secretary*

NATIONAL BUREAU OF STANDARDS
A. V. Astin, *Director*

# THE NATIONAL BUREAU OF STANDARDS

The scope of activities of the National Bureau of Standards at its major laboratories in Washington, D.C., and Boulder, Colo., is suggested in the following listing of the divisions and sections engaged in technical work. In general, each section carries out specialized research, development, and engineering in the field indicated by its title. A brief description of the activities, and of the resultant publications, appears on the inside of the front cover.

WASHINGTON, D.C.

ELECTRICITY. Resistance and Reactance. Electrochemistry. Electrical Instruments. Magnetic Measurements. Dielectrics.

METROLOGY. Photometry and Colorimetry. Refractometry. Photographic Research. Length. Engineering Metrology. Mass and Scale. Volumetry and Densimetry.

HEAT. Temperature Physics. Heat Measurements. Cryogenic Physics. Rheology. Molecular Kinetics. Free Radicals Research. Equation of State. Statistical Physics. Molecular Spectroscopy.

RADIATION PHYSICS. X-Ray. Radioactivity. Radiation Theory. High Energy Radiation. Radiological Equipment. Nucleonic Instrumentation. Neutron Physics.

CHEMISTRY. Surface Chemistry. Organic Chemistry. Analytical Chemistry. Inorganic Chemistry. Electrodeposition. Molecular Structure and Properties of Gases. Physical Chemistry. Thermochemistry. Spectrochemistry. Pure Substances.

MECHANICS. Sound. Pressure and Vacuum. Fluid Mechanics. Engineering Mechanics. Combustion Controls.

ORGANIC AND FIBROUS MATERIALS. Rubber. Textiles. Paper. Leather. Testing and Specifications. Polymer Structure. Plastics. Dental Research.

METALLURGY. Thermal Metallurgy. Chemical Metallurgy. Mechanical Metallurgy. Corrosion. Metal Physics.

MINERAL PRODUCTS. Engineering Ceramics. Glass. Refractories. Enameled Metals. Constitution and Microstructure.

BUILDING RESEARCH. Structural Engineering. Fire Research. Mechanical Systems. Organic Building Materials. Codes and Safety Standards. Heat Transfer. Inorganic Building Materials.

APPLIED MATHEMATICS. Numerical Analysis. Computation. Statistical Engineering. Mathematical Physics.

DATA PROCESSING SYSTEMS. Components and Techniques. Digital Circuitry. Digital Systems. Analog Systems. Applications Engineering.

ATOMIC PHYSICS. Spectroscopy. Radiometry. Mass Spectrometry. Solid State Physics. Electron Physics. Atomic Physics.

INSTRUMENTATION. Engineering Electronics. Electron Devices. Electronic Instrumentation. Mechanical Instruments. Basic Instrumentation.

Office of Weights and Measures.

BOULDER, COLO.

CRYOGENIC ENGINEERING. Cryogenic Equipment. Cryogenic Processes. Properties of Materials. Gas Liquefaction.

IONOSPHERE RESEARCH AND PROPAGATION. Low Frequency and Very Low Frequency Research. Ionosphere Research. Prediction Services. Sun-Earth Relationships. Field Engineering. Radio Warning Services.

RADIO PROPAGATION ENGINEERING. Data Reduction Instrumentation. Radio Noise. Tropospheric Measurements. Tropospheric Analysis. Propagation-Terrain Effects. Radio-Meteorology. Lower Atmosphere Physics.

RADIO STANDARDS. High frequency Electrical Standards. Radio Broadcast Service. Radio and Microwave Materials. Atomic Frequency and Time Standards. Electronic Calibration Center. Millimeter-Wave Research. Microwave Circuit Standards.

RADIO SYSTEMS. High Frequency and Very High Frequency Research. Modulation Research. Antenna Research. Navigation Systems. Space Telecommunications.

UPPER ATMOSPHERE AND SPACE PHYSICS. Upper Atmosphere and Plasma Physics. Ionosphere and Exosphere Scatter. Airglow and Aurora. Ionospheric Radio Astronomy.

USCOMM-NBS-BL


NBS